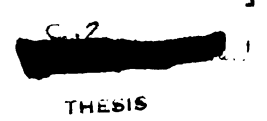
STRESS-STRAIN RELATIONSHIPS FOR SOIL WITH VARIABLE LATERAL STRAIN

Thesis for the Degree of Ph. D.

MICHIGAN STATE UNIVERSITY

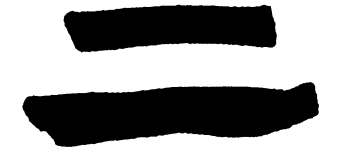
Osamu Kitani

1966





MICHIGAN STATE UNIVERSITY LIBRARY



DEL. 1371 MAR 171972

> MICHIGAN STATE UNIVERSITY LIBRARY



ABSTRACT

STRESS-STRAIN RELATIONSHIPS FOR SOIL WITH VARIABLE LATERAL STRAIN

by Osamu Kitani

A two-dimensional stress-strain law for soil is required for calculations of the general behavior of soil under load or when deformed.

A study was made to investigate the behavior of a cylindrical soil sample which was axially compressed and laterally confined with springs of various spring rates. This kind of test has more similarity to the actual situation where soil expands laterally under increasing axial stress, and the lateral confinement stress is not a constant but a function of the lateral strain. Moreover, even a very loose soil can be tested by this simple and rather inexpensive method.

The soil sample was compressed at a constant speed, and the axial stress, axial strain and lateral strain were measured. The lateral stress was calculated from the test data. Shear strain was obtained from X-ray pictures of lead spheres buried in the soil sample.

A loam with an average moisture content of 12.4% dry basis was used with an average initial bulk density of 0.0346 lb/in³. A friction reducer was applied on the surface of the sample and the wall friction was made small

enough to satisfy the assumptions of uniform stress-strain distribution and negligible shear stress along the wall.

Tests were carried out for the four variable spring rates (lb/in) of 9.6, 56, 264 and ∞ (fixed wall). From the test results, relationships between the two principal stress components and the two principal strain components were determined in graphical form. It was also found that there was an approximately linear relationship between axial stress and lateral stress in the test range of $\epsilon_1 < 0.36$ and $\epsilon_2 < 0.029$.

The functional forms of the relationships between principal stresses and strains were derived by applying the isotropic hardening theory and by modifying it. The functions were of the following form;

$$\sigma_1 = a(\epsilon_1 - 2\epsilon_2)^n$$

The maximum shear stress was not a function of the maximum shear strain alone, but was linearly related to the mean normal stress.

The functional relationship between the mean normal stress and the volume change (or the bulk density) was also derived.

Approved

Major Professor

Approved

Department Chairman

STRESS-STRAIN RELATIONSHIPS FOR SOIL WITH VARIABLE LATERAL STRAIN

Ву

Osamu Kitani

A THESIS

Submitted to
Michigan State University
in partial fulfillment of the requirements
for the degree of

DOCTOR OF PHILOSOPHY

Department of Agricultural Engineering

ACKNOWLEDGMENTS

The author expresses his sincere gratitude to his major professor Dr. P. E. Sverker Persson for the guidance throughout his study.

To the other members of guidance committee, Dr. B. A. Stout, Agricultural Engineering Department, Dr. G. E. Mase, Metallurgy, Mechanics and Material Science Department, and Dr. O. B. Andersland, Civil Engineering Department, the author wishes to express his gratitude for their valuable suggestions and help.

Dr. L. E. Malvern, Metallurgy, Mechanics and Material Science Department gave many valuable theoretical suggestions and advice to the author. Dr. S. Serata, Civil Engineering Department gave important suggestions on the experimental phase.

Gratitudes are also expressed to the Fulbright Commission in Japan which delegated the author as an exchange visitor to the United States.

Mr. J. B. Cawood and his staff in the Agricultural Engineering Research Laboratory assisted in the development of the experimental apparatus. Dr. U. V. Mostosky and Miss D. L. Middleton in Veterinary Clinic provided the author

with X-ray machine and gave assistance. Mr. J. D. Wilson helped in revising the manuscript.

This dissertation is dedicated to my wife Shigeko.

TABLE OF CONTENTS

																Page
ACKNOW	LEDGM	ENTS	•	•	•	•	•	•	•	•	•	•	•	•	•	11
LIST O	F FIG	URES	•	•	•	•	•	•	•	•	•	•	•	•	•	vi
LIST O	F TAB	LES A	ND	APF	ENI	OICE	S	•	•	•		•	•	•	•	vii
LIST O	F SYM	BOLS	•	•	•	•	•	•	•	•	•	•	•	•	•	ix
ı.	INTR	ODUCI	OI	1.	•	•	•	•	•	•	•	•	•		•	1
II.	REVI	EW OF	L	TEF	J'TAS	JRE	•	•	•	•	•	•	•	•	•	3
		2.1						Defo ngth				tud •	y	•	•	3 10
III.	THE	PROBI	EM	•	•	•	•	•	•		•	•	•	•	•	12
		3.1 3.2								ly	•	•	•	•	•	12 13
IV.	EXPE	RIMEN	IAT	L AI	PAF	RATU	JS A	AND	PRO	CED	URE		•	•	•	16
		4.1 4.2		par coce			•	•	•	•	•	•		•	•	16 23
v.	METH	OD OI	7 A1	VAL	SIS	3.		•	•	•	•	•	•	•		28
		5.1 5.2						rain tres						•	•	28
		-	S	Stre	88	and	l Vo	olun	ne C	han	ge	•	•	•	•	32
VI.	RESU	JLTS	•	•	•	•	•	•	•	•	•	•	•	•	•	3 5
		6.1 6.2 6.3 6.4	F σ σ τ	ar l Ve l Ver	nd I ersu ersu rsu	F ₂ I ls e ls c	und 1 1 72 1 Re	lts ctic Rela Rela lati	ns ations	nsh nsh ship	ip ip	•	•	•	•	35 39 41 46
		6.6	σı	n ve	ersi	as $\bar{7}$	$\frac{1}{70}$	Rela	at 10	nsh	ıp	•	•	•	•	46

															Page
VII.	DISC	JSSIO	N .	•	•	•	•	•	•	•	•	•	•	•	53
		7.1	Str	air	-ha	rde	nin	g T	heo	ry	and	Fı			
			and	\mathbf{F}_2	Fu	nct	ion	8.	•	•	•	•	•		53
		7.2													64
		7.3												•	66
		7.4										and .			67
			Mac	MI.6	II D	or.a	4 11	ay a	Cem	•	•	•	•	•	01
VIII.	SUGGI	ESTIO	ns f	OR	THE	AP	PLI	CAT	ION	s.	•	•	•	•	71
IX.	SUMM	ARY A	ND C	ONC	LUS	ION	s.	•	•	•	•	•	•	•	73
		9.1	Sum	mar	у.	•	•	•	•	•	•	•	•	•	73
		9.2	Con	clu	sio	ns	•	•	•	•	•	•	•	•	75
SUGGEST	rions	FOR	FUTU	RE	STU	DY	•	•	•		•	•	•	•	78
REFERE	ICEC														79
VELEVEL	1CES	• •	•	•	•	•	•	•	•	•	•	•	•	•	13
APPEND	rx .		_	_	_						_		_		81

LIST OF FIGURES

Figure		Page
2-1. 2-2.	Stress-Strain Relations for Soil Stress-Strain Curves from Soehne's Tests	4 8
4-1. 4-2.	General View of Test Device	17 18
4-3. 4-4.	Compression Device	20
h e	Recorders	22
4-5. 4-6.	Soil Specimen after Compression (Covered with a thin plastic film sandwiched by the friction	25
4-7.	reducer)	25 27
5-1.	Dimensions of the Soil Specimen and the Stress-	-
	Strain Components	29
5-2.	Shear Strain	3 3
5-3.	Calculation of γ_{π} from e_1 and e_2	33
6-1.	X-Y Records for Three Tests for Each of Four	
_	Spring Rates	36
6-2.	σ_1 versus ε_2 and ε_1 Relationship	37
6-3.	σ_2 versus ε_2 and ε_1 Relationship	38
6-4.	σ_1 versus ε_1 Relationship	40
6-5.	$\log \sigma_1$ versus $\log \varepsilon_1$ Lines	42
6-6.	$\log \sigma_1$ versus ε_1 Curves	43
6-7.	σ_1 versus σ_2 Relationship	44
6-8.	γ Values from X-ray Test and from e_1 and e_2 .	47
6-9.	τ versus γ Relationship	48
6-10.		49
6-11.	$\log \sigma_{m}$ versus $\log \Delta V/V_{0}$ Relationship	50
6-12.	$\log \sigma_{m}^{-}$ versus $\Delta V/V_{0}$ Relationship	51
7-1.		
7-2.	σ_1 from the Modified Equation (1)	59
7-3.	σ_1 from the Modified Equation (2) $\eta = 1$	61
7-4.	σ_2 from the Modified Equation (2) $\eta = 1$	62
7 - 5.	$\log (\sigma_1 - \sigma_2)$ versus $\log (\epsilon_1 - 2\epsilon_2)$ relation-	_
_	ship	63
7-6.	σ_1 from the Modified Equation (2) $\eta = 1/2$	65
7-7.	σ_m Calculated from $\Delta V/V_0$	68
7-8.	log σι versus log eι Relationship	69

LIST OF TABLES AND APPENDICES

Table		Page
6-1. µ	= σ_2/σ_1 Values	45
Λppendix		
A-1.	Calibration Chart for Axial Force Trans-ducer	82
A-2.	Calibration of Axial Displacement of Compression Piston in Terms of Time	83
A-3.	Spring Constants k	83
A-4.	Calibration Chart for Lateral Displacement Transducer	84
B-1.	σ_1 Values	85
B-2.	e_1 and ϵ_1 Values	86
B-3.	σ ₂ Values	87
B-4.	e_2 and ϵ_2 Values	88
B-5.	σ_m , σ_1 ', and σ_2 ' Values	89
B-6.	τ_{π} Values	90
B-7.	γ Values	90
B-8.	$ au$ $\Delta extstyle au$ Values	91
B-9.	μ Values Calculated from Individual Test .	92
C-1.	σ ₁ Values from Isotropic Hardening Theory.	93
C-2.	σ_1 Values from the Modified Equation (1) .	93
C-3.	σ_1 Values from the Modified Equation (2),	94

Appendix		Page
C-4.	σ_2 Values from the Modified Equation (2), $\eta = 1 \dots \dots$	94
C-5.	σ_1 Values from the Modified Equation (2), $\eta = 1/2$	95
C-6.	$\tau_{\mathfrak{m}}/\sigma_{\mathfrak{m}}$ Values	96
C-7.	σ_m^4 Values Calculated from $\Delta V/V_0$	96
C-8.	Comparison Between Conventional Strain System and Natural Strain System	97

LIST OF SYMBOLS

- A current section area of soil specimen.
- A₀ initial section area of soil specimen.
- a soil parameter; $\sigma_1 = a(\epsilon_1 2\epsilon_2)^n$
- c cohesion
- d rate of deformation
- e₁ conventional axial strain
- e₂ conventional lateral strain
- F_1 σ_1 function; $\sigma_1 = F_1(\varepsilon_1, \varepsilon_2)$
- F_2 σ_2 function; $\sigma_2 = F_2(\varepsilon_1, \varepsilon_2)$
- G τ function; $\tau = G(\gamma)$
- H function of volume change in terms of mean normal stress
- H_{I} strain-hardening function; $\overline{\sigma} = H_{T}(\overline{\epsilon})$
- k spring constant
- current length of soil specimen
- \mathfrak{L}_0 initial length of soil specimen
- At axial displacement (change of length of specimen)
- Δ12 tangential displacement
- n soil parameter; $\sigma_1 = a(\epsilon_1 2\epsilon_2)^n$
- P₁ axial force
- P₂ lateral force (spring force)
- r current radius of soil specimen
- r₀ initial radius of soil specimen

- ar increment of radius
- s shear stress (ultimate value)
- t time (time of compression)
- V current volume of soil specimen
- V initial volume of soil specimen
- ΔV change of volume; $\Delta V < 0$ for compression
- y shear strain
- ε₁ natural axial strain
- ε₂ natural lateral strain
- η contribution factor of ϵ_2 to ϵ_1
- angle of inclination of plane from the maximum principal stress direction
- μ soil parameter $\mu = \sigma_2/\sigma_1$
- v Poisson's ratio:
- p bulk density
- σ_1 axial stress
- σ₂ lateral (radial) stress
- σ₁' deviatoric axial stress
- σ2' deviatoric lateral stress
- $\sigma_{\rm m}$ mean normal stress; $\sigma_{\rm m} = \frac{\sigma_1 + 2\sigma_2}{3}$ for cylindrical case
- τ shear stress
- angle of internal friction
- generalized strain; $\frac{1}{\epsilon} = \sqrt{\frac{2}{3}} \epsilon_{ij} \epsilon_{ij}$
- $\bar{\sigma}$ generalized stress; $\bar{\sigma} = \sqrt{\frac{3}{2} \sigma'_{1,1} \sigma'_{1,1}}$
 - On p. 6, 7, and 10, $\overline{\sigma}$ is used as the effective stress in soil.

I. INTRODUCTION

The stress-strain relationship of soil is the most important basis for all the problems related to the soil deformation and failure.

The problem of tillage, in which one of the important objectives is how to reduce the draft and the tillage energy, can only be solved completely after the stress-strain law of soil is established and whereby the draft and the energy for various tillage tools under certain soil conditions can be calculated.

The traction problems also require the knowledge about the stress-strain law. To achieve maximum traction, the soil deformation and the stress under the tractor tire or shoe must be calculated. The integration of the stress along the border will yield the traction force which we want to maximize.

Thus, agricultural engineers need soil stress-strain relationship which can be applied to the practical problems, or at least, can be a basis for them. The main effort in this thesis has been devoted to get a stress-strain relationship of soil which is applied to the practical problems.

Agricultural engineers have rather special problems in the study of stress-strain laws of soil, because the soils on the field surface are soft and highly compressible. Accordingly they are work-hardened very much. They also contain complex organic matter. These features create different problems from those in foundation engineering in which the engineers are mainly interested in compacted soils.

II. REVIEW OF LITERATURE

There are two main categories in the study field of soil stress-strain relations. They are the study of force versus deformation and the study of ultimate strength which may be considered as a part of stress-strain relationship in the form of yield criterion.

2.1 Force versus Deformation Study

Soil changes its rheological properties according to its texture, moisture content and density as well as loading history. Therefore, there are several ways of approach in this field. The theoretical studies so far have been based upon theories of either elasticity, plasticity or viscoelasticity.

The theory of linear elasticity has been used quite extensively in foundation engineering especially as the means of calculating initial settlement. It is assumed that the strain is completely recoverable and it follows the linear stress-strain relationship as shown in Fig. 2-1 (a-1). In a 3-dimensional case it is written in the following form.

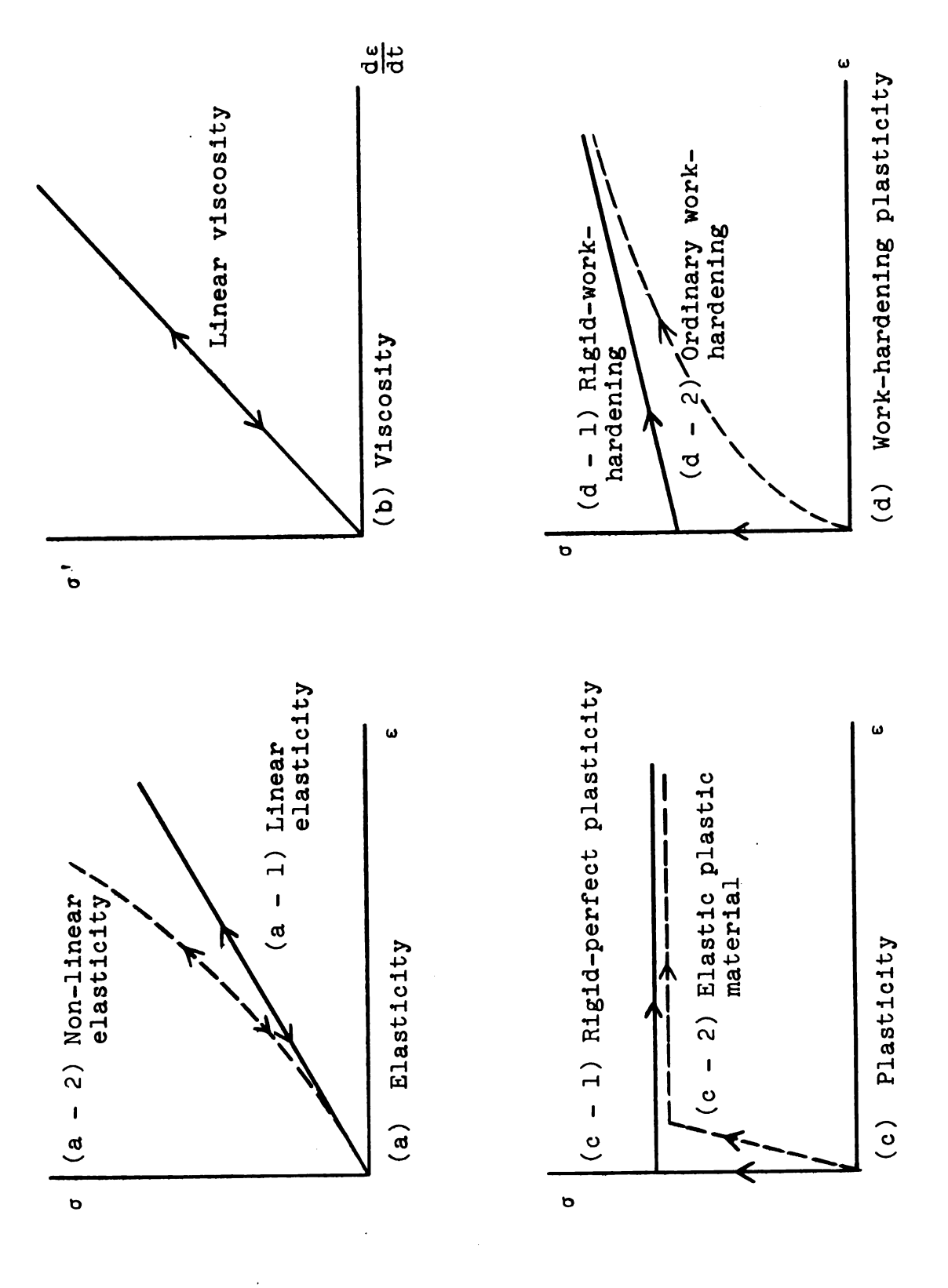


Fig. 2-1. Stress-Strain Relations for Soil

$$\varepsilon_{x} = \frac{1}{E} \{ \sigma_{x} - \nu (\sigma_{y} + \sigma_{z}) \}$$

$$\gamma_{xy} = \frac{1}{G} \tau_{xy}$$
(2.1)

where E, G and v are constants.

The agricultural soils are mostly so soft that it is impossible to assume a complete recovery of strain after the external force has been removed. Soehne: (1956) reported that the surface soil behaved as a non-linear elastic material (broken line in Fig. 2-1 (a)) only after it was repeatedly loaded up to the highest load encountered.

Thus, the surface soils have quite plastic characteristics. Only particular types of clay of certain moisture content do, however, show nearly ideal plastic flow which is defined

$$s_{x} = \frac{K}{\sqrt{II_{d}}} d_{x} \qquad etc. \qquad (2.2)$$

where s_{χ} is shear stress or deviatoric stress K is a constant which represents yield value

II_d is the second invariant of rate of deformation

 d_{x} is rate of deformation.

This relation corresponds to either one of the flat lines in Fig. 2-1(c).

By assuming rigid-perfect plasticity with the yield criterion in the form of Coulomb's equation, we can calculate

^{*}etc. means similar equations for y and z components.

stress-strain distribution of hard (incompressible) soil under simple boundary conditions as described by Scott (1963) b. 510.

Berezantsev (1955) analyzed the soil deformation under a conical head by means of the plastic equilibrium theory of soil.

However the actual situation is far more complex. Soil shows work-hardening due to the increase of strain (and stress) as shown in Fig. 2-1(d). Drucker et al. (1957) showed that soil should be treated as a work-hardening material. Drucker (1961) also tried to apply limit analysis to soil.

In many cases, efforts have been made to get a stress-strain relationship of soil as a mixture of non-linear elasticity and some kind of plasticity through simulation type tests. That is to say, strain remains even after the load is removed, sometimes no yield point is reached, or even if it reaches the yield point, stress does not necessarily remain constant.

Actually most of the studies do not consider the factor of time. They take into consideration only stress and strain in the same manner as elasticity. The most frequently used relationship of this kind is the consolidation equation.

$$\Delta e = e_0 - e = c_0 \log \frac{\overline{\sigma}}{\overline{\sigma}_0}$$
 (2.3)

where e is void ratio, c_c is a constant. If one-dimensional consolidation is assumed, eq. (2.3) can be written in the form of the following stress-strain relation.

$$\epsilon_{\mathbf{x}} = \mathbf{c} \log \overline{\sigma} + \mathbf{c}'$$
 (2.4)

Roberts and Souza (1958) reported that this relationship was valid also for the very high stress under which the soil particles themselves are crushed.

Another equation of this type is Bekker's sinkage equation which has been used in traction problems. The relationship between penetration pressure p and sinkage z under a penetration disk is described as

$$p = Kz^n \tag{2.5}$$

where K and n are constants.

If one-dimensional situation is assumed for eq. (2.5), it becomes

$$\sigma_{\mathbf{X}} = K \epsilon_{\mathbf{X}}^{\mathbf{n}} \tag{2.6}$$

In the lower axial force range, the axial force versus displacement curve of Soehne's study (1956) plotted by the author in Fig. 2-2, shows itself in the form of Bekker's equation, whereas, in the higher range it obeys the consolidation law. Soehne's soil compression tests were carried out in a rigid wall cylinder.

Another stress-strain relationship which has recently been studied extensively is the viscoelastic theory which

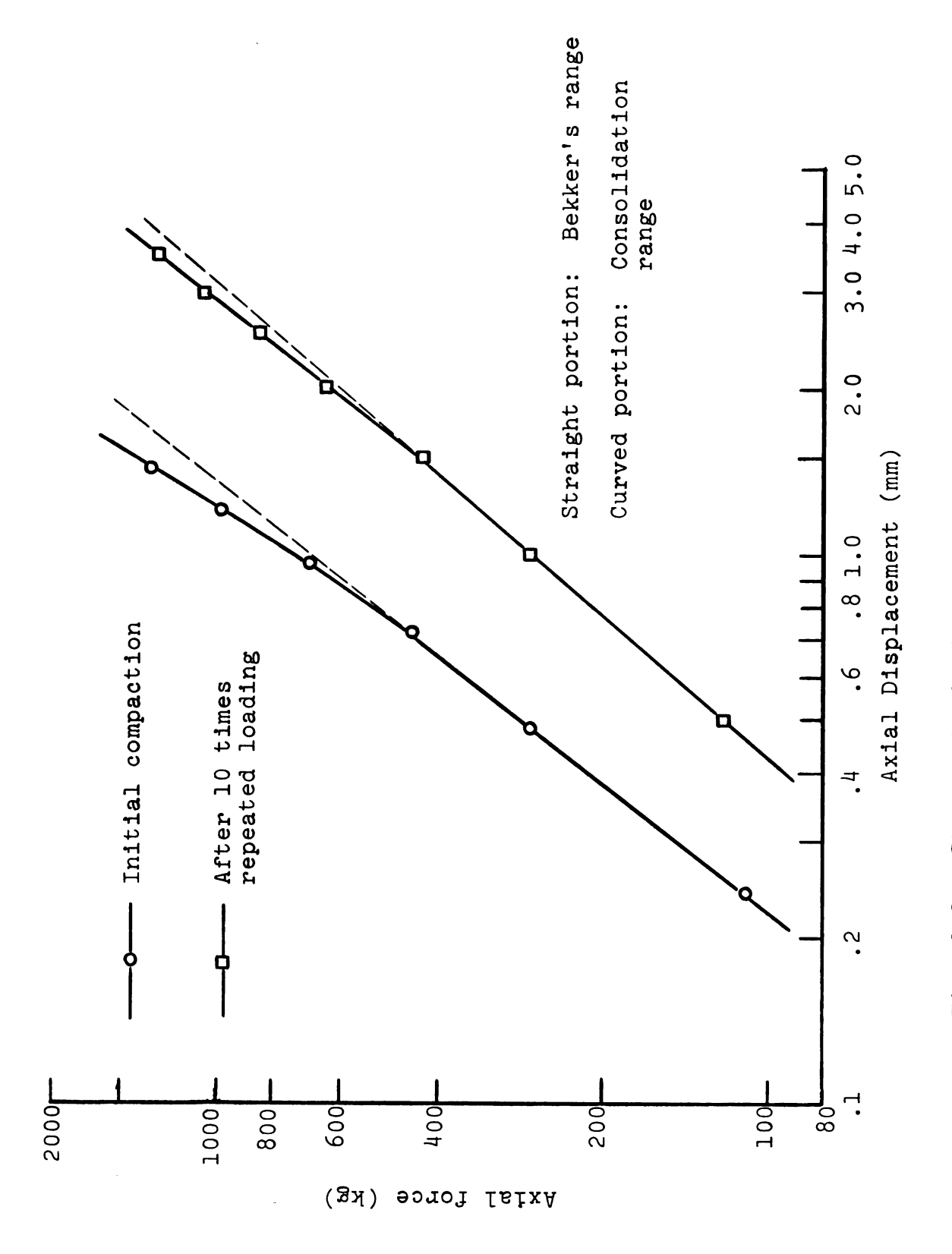


Fig. 2-2. Stress-strain Curves from Soehne's Tests

is a combination of (a-1) and (b) in Fig. 2-1 and expressed in the following form.

$$s_{xy} = G \gamma_{xy} + \eta \frac{d\gamma_{xy}}{dt} \quad \text{etc.}$$
 (2.7)

where G and n are constants.

McMurdie (1963) carried out a set of triaxial tests and creep tests. He reported that the viscoelastic theory agreed best with the test results.

Kondner and Krizek (1964) have developed a vibratory soil compression test device with which they analyzed the soil behavior and divided the strain into the storage part and the dissipation part.

Waldron (1964) showed that the strain super-position law of viscoelastic theory is valid for soils only within a limited range of moisture content, stress and time. He also obtained three viscoelastic functions from his tests.

There are some studies which do not deal with the constitutive laws of soil, but rather check whether or not some stress-strain relation of continuous media is valid for soil. VandenBerg et al. (1958) suggested that the bulk density change during soil compaction should be caused only by mean normal stress. However, VandenBerg (1962) later reported that the triaxial tests with diametral measurement showed that the change in bulk density ρ is not a function of mean normal stress σ_m alone but also a function of maximum shear strain $\overline{\gamma}_{max}$ in the following exponential form.

$$e^{a\rho - b} = \sigma_{m}(1 + \overline{\gamma}_{max}) \tag{2.8}$$

where a, b are constants.

2.2 <u>Ultimate Strength Study</u>

Many studies have been carried out from the viewpoint of soil strength based upon the famous Coulomb's law.

$$s = c + \overline{\sigma} \tan \phi \tag{2.9}$$

where s is ultimate shear strength, c is cohesion and ϕ is angle of internal friction.

Hendrick and VandenBerg (1961) conducted a tensile strength test of soil at various loading rates and obtained c values at tensile failure. They concluded that the ultimate strength does not change with a change in the loading rate, whereas the deformation at failure decreases as loading rate increases.

Vomocil et al. (1961) carried out a tensile test using centrifugal force.

The triaxial test is considered as the most reliable test to measure the two parameters c and \$\phi\$. Normally soil fails in a progressive manner. In the case of a triaxial test the stress condition, however, changes rapidly with the increase of deformation, especially after maximum stress is reached. To avoid this, other devices such as torsion shear apparatus have been developed (for example, Waterway Experiment Station, 1952).

Some people tried to combine deformation and ultimate strength laws together. Taylor and VandenBerg (1965) introduced deformation J in the failure equation.

$$s = c + \sigma^{1-n} J^n K$$
 (2.10)

where n and K are constants.

They derived this formula from a series of tests with a ring shear device in laboratory soil.

III. THE PROBLEM

3.1 Purpose of Study

As described in the previous chapter, several stressstrain laws for soil have been proposed for the one-dimensional case. However a two-dimensional stress-strain
relationship is required to solve the practical problems
of tillage and traction, because in soils their strength
as well as their stress-strain level depends largely on
the mean normal stress. This indicates that the stressstrain relationships of soil, unlike those of metals,
could be largely affected by the mean normal stress. The
particular problem of this study may be defined as describing how the relationship between axial stress and axial
strain in a compression test of a cylindrical soil specimen
is affected by the lateral (radial) stress and lateral strain.

This kind of study with various lateral stresses can be carried out with a triaxial compression test apparatus with lateral strain pick-up. The triaxial test is, however, limited to those soils with a certain natural strength so that the sample can maintain its shape without lateral support. This is a great disadvantage for studying stress-strain relationships of a soft surface soil in agriculture. For these, it is necessary to provide lateral support for the

soil specimen. This kind of device could be used even for a very loose sand.

The triaxial test also takes time to be carried out.

It requires rather expensive equipment. A test device with lateral confinement can be much simpler, because it does not require handling the soil specimen in liquid.

Moreover some of the practical problems of tillage and traction have boundary values in terms of strain rather than stress, for example, boundary by a rigid blade or an elastic tire. In this situation, a test with various types of strain confinement may be more suitable than a stress confinement test. More generally, almost any element of soil under load in one direction is subjected to a confinement in the other direction, where the confinement stress is not a constant but a function of the lateral strain. Because the soil strength is affected by this lateral stress and strain, a realistic testing should be made with a strain-defined lateral confinement.

3.2 Assumptions for Study

Thus, a soil compression test in which lateral strain confinement is controlled was designed. Actually the lateral confinement was provided by two springs. There is, therefore, an approximately linear relationship between lateral stress and lateral strain as; $\sigma_2 = k_2 \varepsilon_2$. (cf. eq. (5.4)). The lateral strain level at a certain axial stress or

axial strain can be controlled through the exchange of springs with various spring constants k.

The test has to be limited to the loading process and to the loads below the failure point. Within these limitations, the stress-strain relationship is considered to be a single valued, monotonically increasing function. Hence, the relationship between normal stress and normal strain in this cylindrical case (or in the general two dimensional case) could be described by the following two functions.

$$\sigma_1 = F_1(\varepsilon_1, \varepsilon_2)$$

$$\sigma_2 = F_2(\varepsilon_1, \varepsilon_2)$$

where σ_1 and σ_2 are principal stresses ε_1 and ε_2 are principal strains

For the measurement of these principal stresses and principal strains as described later, it is assumed that the stress state is uniform in the whole sample and that the principal axes are parallel and perpendicular respectively to the axis of the cylinder. In order for this to be true the assumption that there is no wall friction must be satisfied.

The shear stress can be calculated from the principal stresses σ_1 and σ_2 assuming homogeneity of the soil. The shear strain is picked up from X-ray pictures of the soil as the change of the angle of a line in the soil.

As the first step, the author assumed that there is a functional relationship between shear stress τ and shear strain γ independent of normal stress and strain components.

$$\tau = G(\gamma)$$

Thus the stress-strain relationship in any two-dimensional case (even when principal components are not known) is fully described by the three functions F_1 , F_2 and G. These functions make it possible to calculate the three stress components if the three strain components are given.

It might also be possible to calculate the stressstrain distribution under certain boundary conditions using the equations of equilibrium, compatibility and boundary values.

The above mentioned two-dimensional approach might be applied to some of the practical three-dimensional problems by further breaking down the problem into numbers of two-dimensional problems.

IV. EXPERIMENTAL APPARATUS AND PROCEDURE

4.1 Apparatus

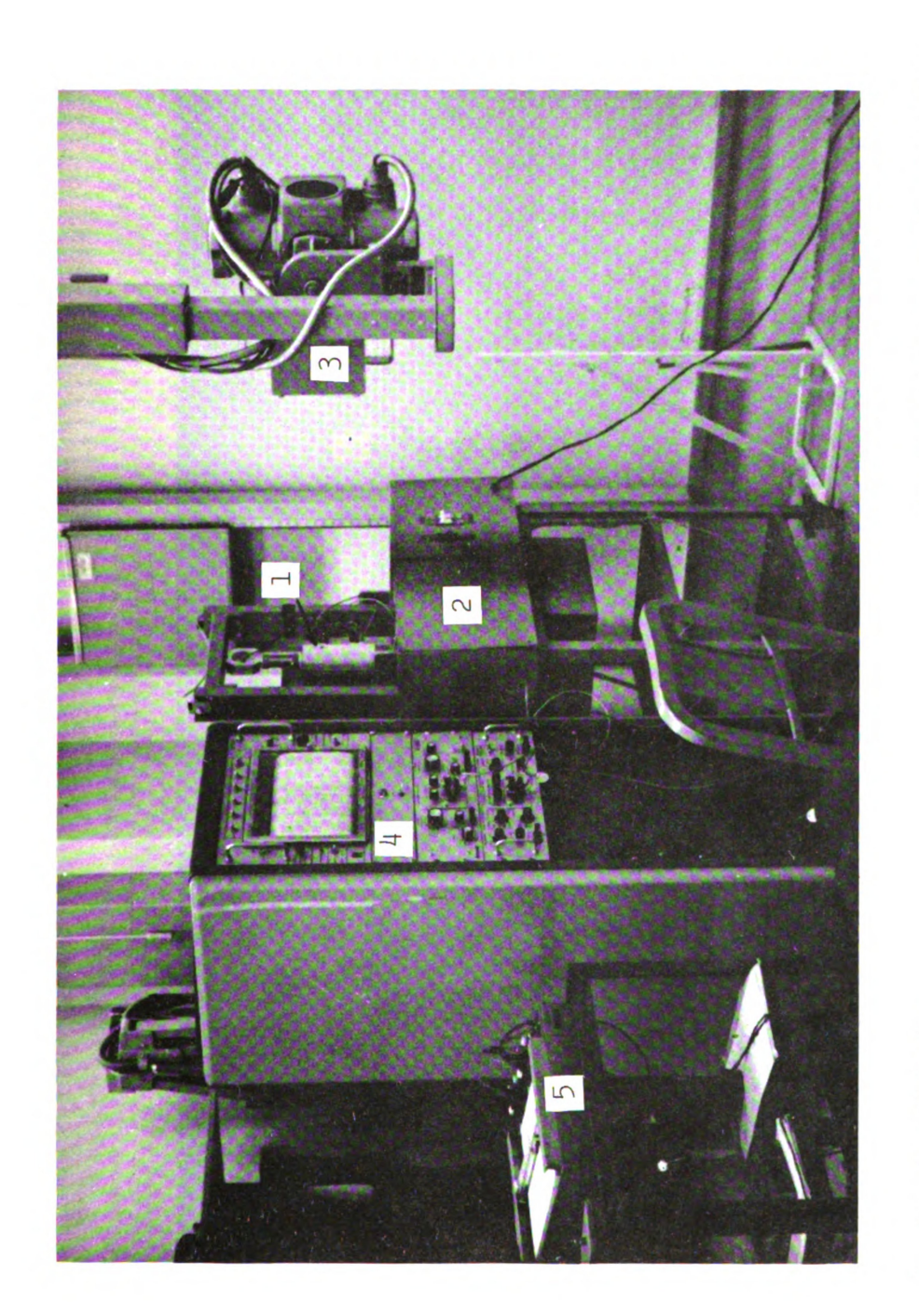
The general view of the test equipment is given in Fig. 4-1. It is composed of a soil compression device, test cylinder, amplifiers, strip-chart recorder, X-Y recorder and X-ray machine.

Compression Device

The soil compression device compresses the cylindrical soil specimen at a constant speed. Three speeds can be selected. The picture of the compression device is given in Fig. 4-2. The designed maximum compression force is 1000 lbs. and the maximum piston stroke is 4.5-inches. The upper and the lower position of the piston is controlled by two limit switches. A 1/4 H.P. induction motor drives the piston screw through two worm gears, a V-belt and a chain.

The axial force transducer is made as a ring of high strength aluminum alloy. Four SR-4 strain gages are attached to the inside wall of the ring. The calibration (App. A-1) shows good linearity.

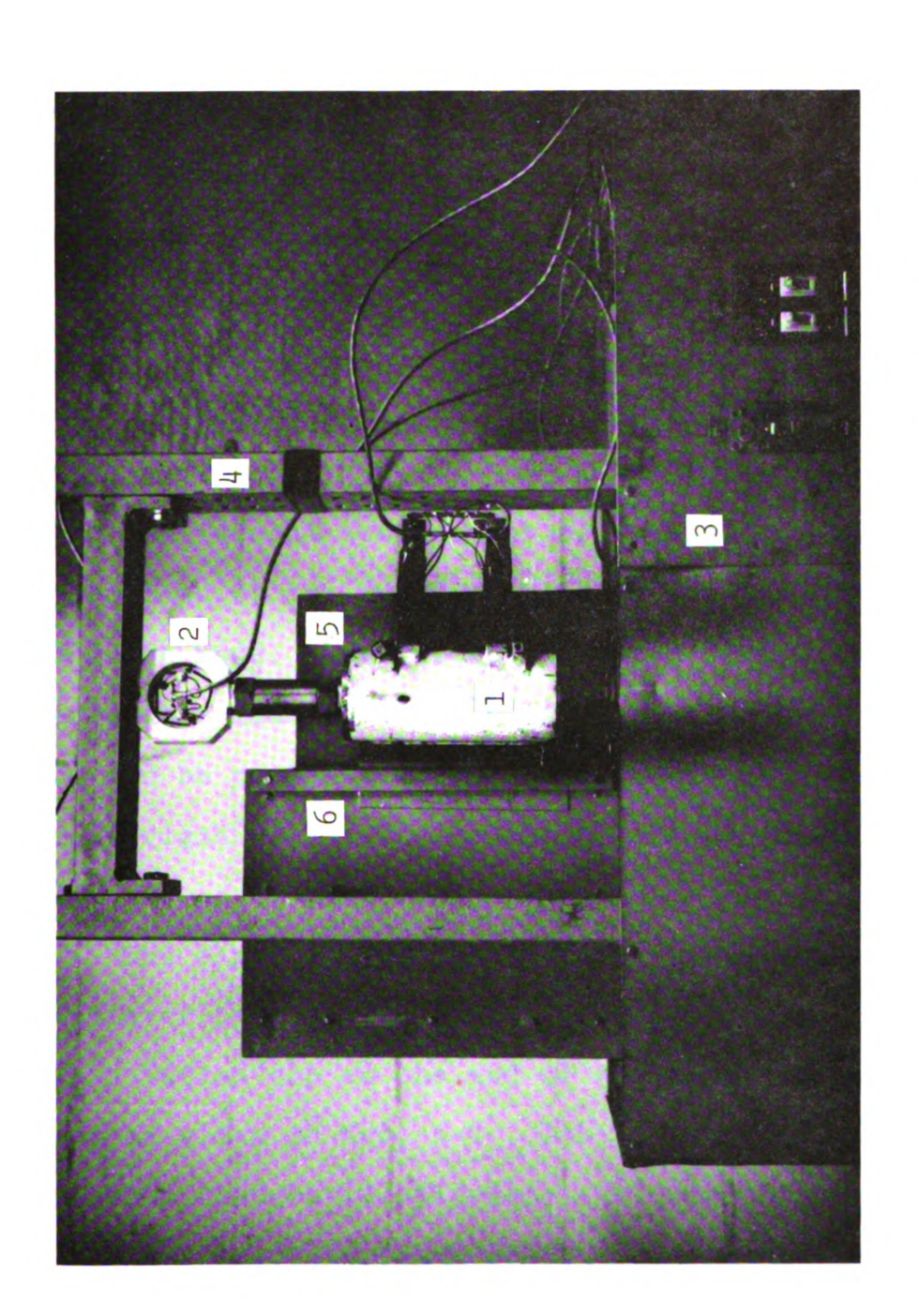
The axial displacement of the piston could be picked up by a strain gage equipped cantilever connected to the driving screw. However, since the axial displacement has



Test cylinder
 Compression device
 X-ray machine

4. Amplifiers and recorder 5. X-Y recorder

General View of Test Device F1g. 4-1.



Test cylinder
 Axial force transducer
 Driving unit box

4. Loading frame5. X-ray film holder6. Lead shield

Fig. 4-2, Compression Device

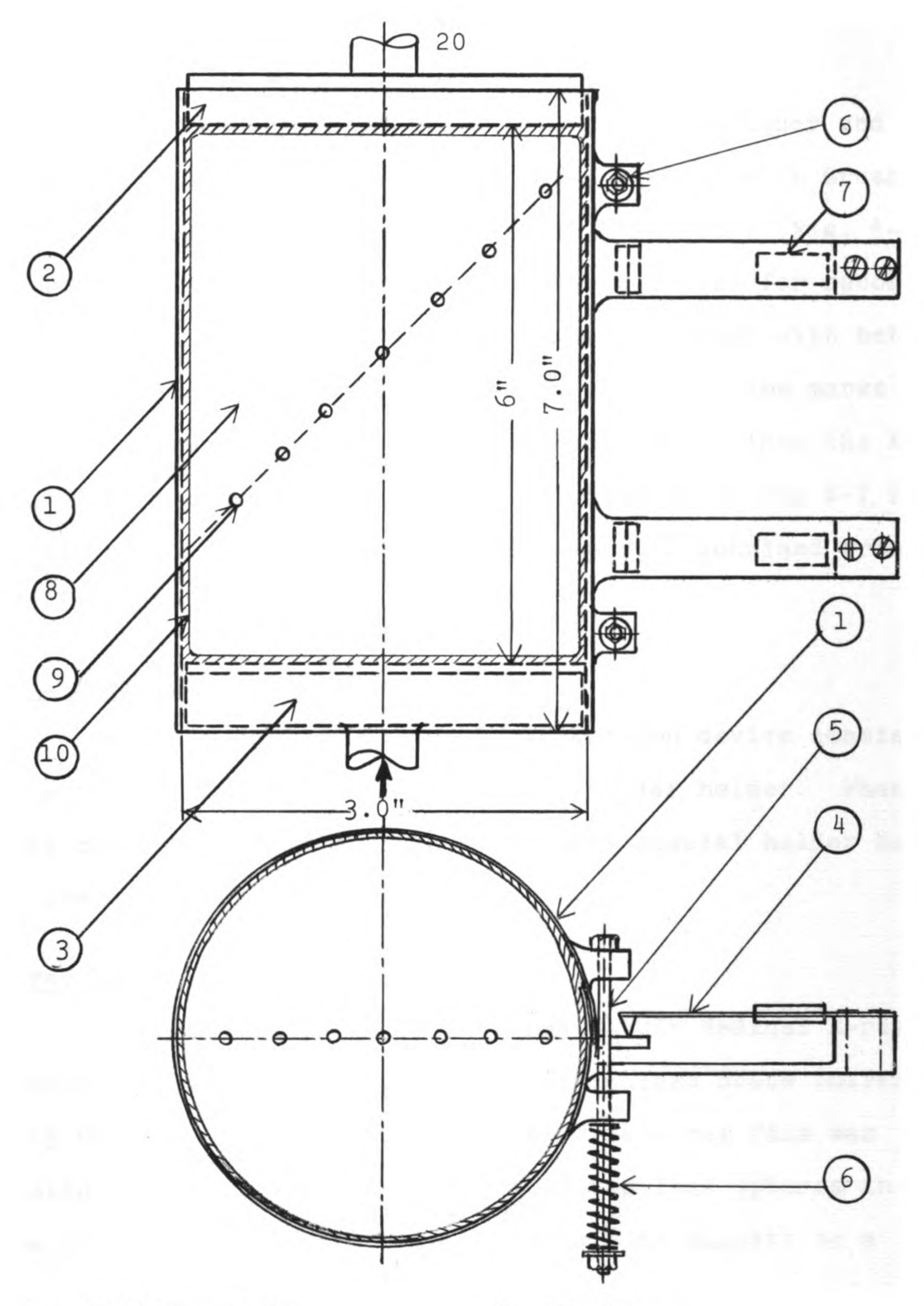
complete linearity in terms of driving time as shown in App. A-2, it is simpler and more accurate to get the axial displacement from the driving time.

Test Cylinder and Stress-Strain Pickup Device

As shown in Fig. 4-3, the test cylinder has an overlapping split side wall. The inside diameter is 3-inches. The height is 7-inches. The cylinder is made of 0.0156inch thick steel plate. The friction in the overlap is reduced by means of a friction reducer which is mentioned later.

The lateral confinement of the soil in the cylinder is provided by two springs which deform tangentially along the guide rods. Several springs with various spring constants were made so that the condition of lateral confinement can be controlled from an almost free expansion to an almost rigid wall. The spring constants are given in App. A-3.

The expansion of the cylinder is measured by the two cantilever type strain gage transducers made of spring steel with a Teflon tip on the end of the beam. The calibration curve is given in App. A-4. The relationship between radial expansion (tangential displacement) and the output reading on the X-Y recorder chart shows fairly good linearity. From the radial expansion the lateral strain of the soil can be calculated.



- 1.
- 2.
- Cylinder wall Upper piston Lower piston Lateral displacement 3. 4. transducer
- Spring guide rod 5.

- 6.
- Springs Strain gages
- Soil 8.
- 9. 10. Lead spheres Friction reducer

Fig. 4-3. Test Cylinder

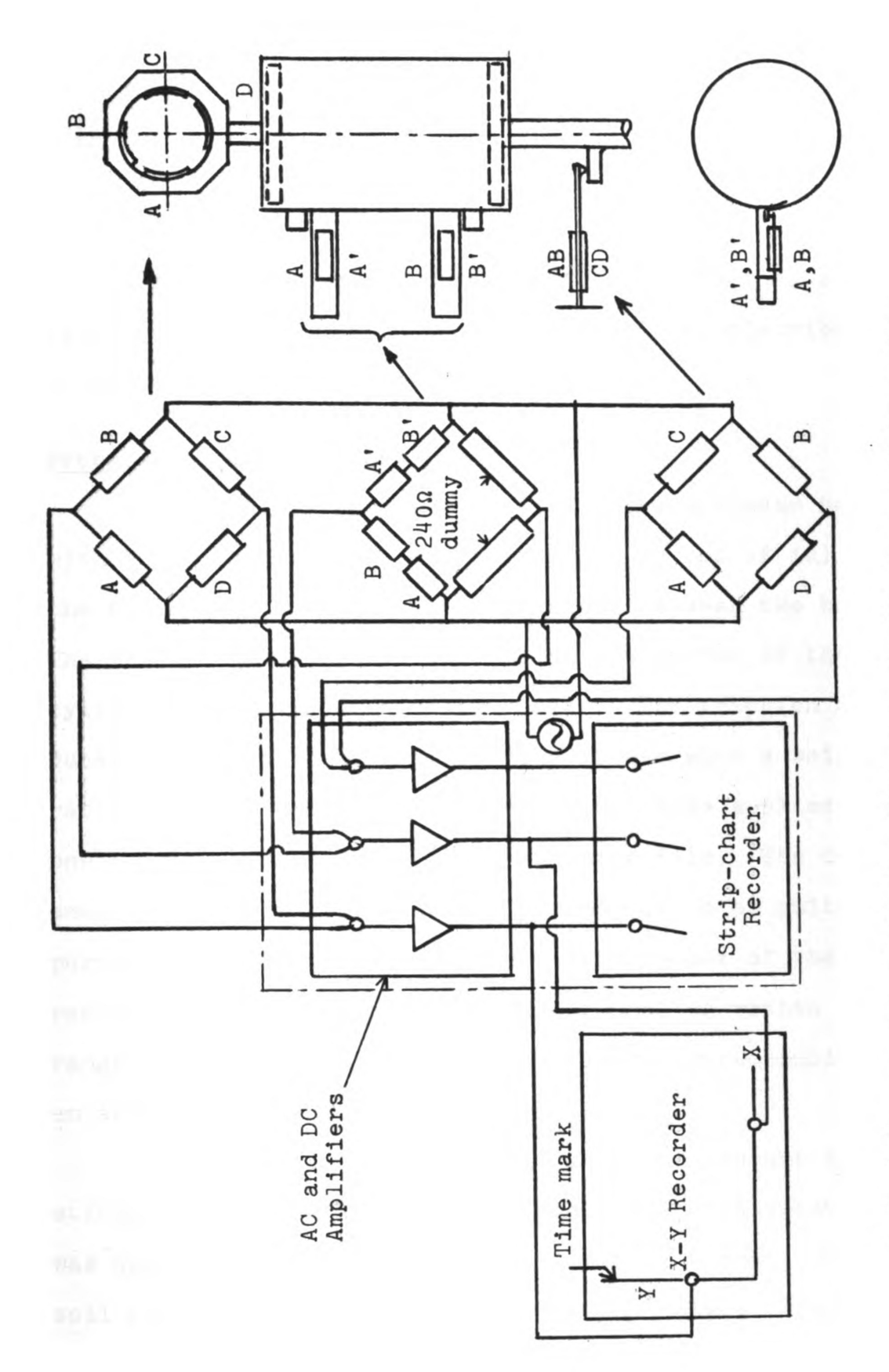
The strain gages on the axial force transducer and lateral displacement transducers are hooked up with Brush RD5612 and BL310 amplifiers and a Brush recorder (Fig. 4-4). In addition a Moseley 135 X-Y recorder was used for recording the axial force and the lateral displacement with better accuracy than the strip-chart recorder. With time marks on the X-Y curve produced by feeding time signals into the X-Y recorder, a complete set of data is obtained on the X-Y recorder chart, because axial displacement is obtained from the time marks.

Soil Preparation Device

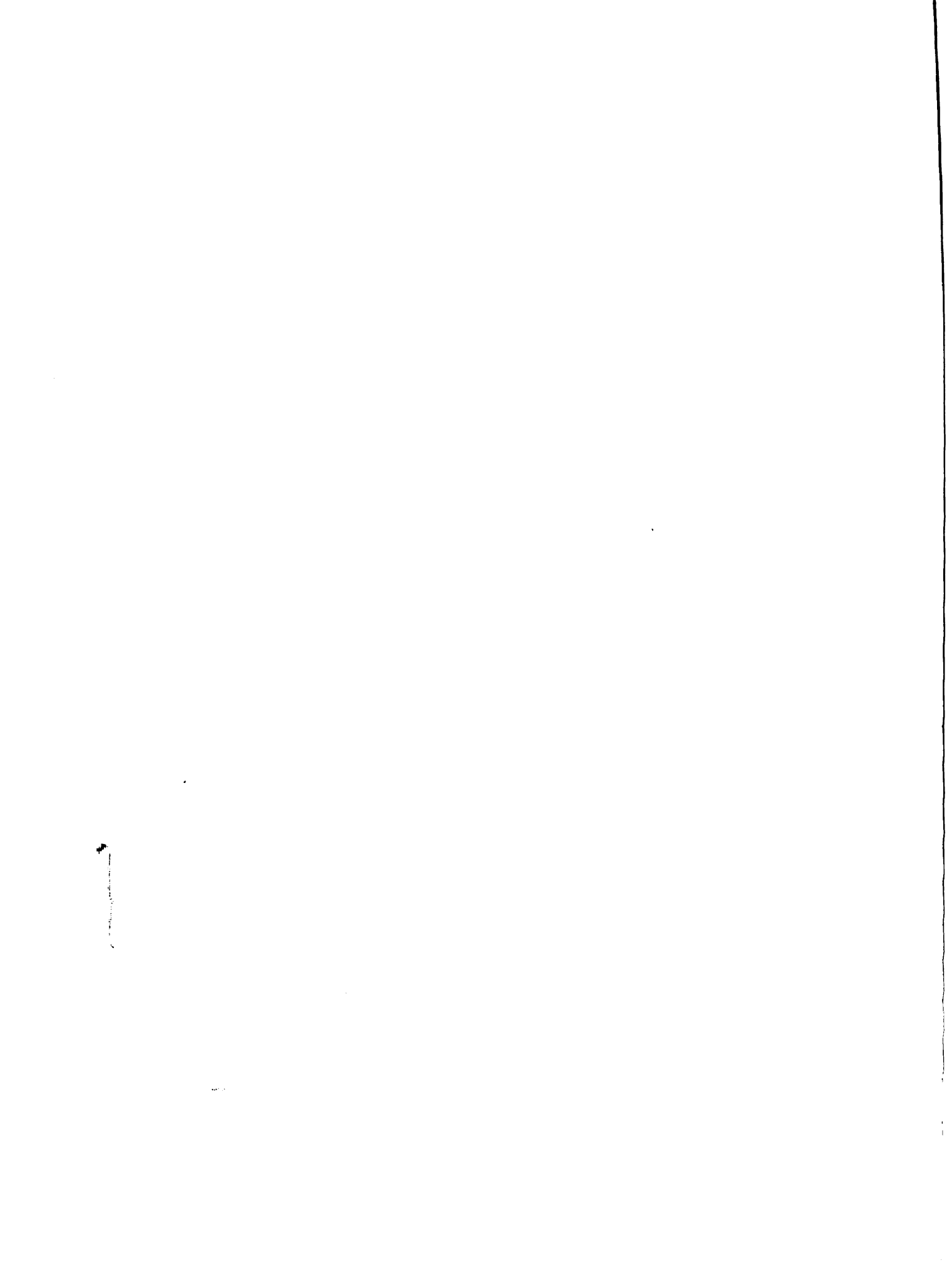
The main part of the soil preparation device consists of a pneumatic vibrator and a test cylinder holder. When lead spheres are buried in a 45° line a special holder base is used as shown in Fig. 4-5.

X-ray Machine

A General Electric Model 11DB6, 150KV Medical X-ray machine in the Veterinary Clinic of Michigan State University was used. Kodak Industrial AA Type X-ray film was chosen to get an accurate picture of the lead spheres in the soil specimen. The film attached with magnets to a plate of steel and a lead shield were placed just behind the test cylinder (Fig. 4-2). To secure an exact distance between the X-ray source and the film a wooden frame was used.



Layout of Strain Pick-ups, Amplifiers, and Recorders Fig. 4-4.



4.2 Procedure

Soil

A loam with average moisture content of 12.4% dry basis (range 11.5-13.0%) was used. The soil was sieved with a 1/4-inch mesh sieve. Then it was kept in a can to keep a constant moisture content and uniform distribution of soil water during a series of tests.

Preparation of Soil Specimen

The test cylinder was placed in the cylinder holder with the piston (and a thin disk plate on top of it) at the bottom of the cylinder and clamped between two holders. The friction reducer was applied on the inside of the cylinder wall with a painting roller. The friction reducer is a mixture of graphite and grease with a weight ratio of 1:3. The friction reducer was also applied on one side of a sheet of plastic wrapping film. The total amount of the friction reducer turned out to be quite important for this test. Therefore, the amount of the friction reducer applied to a specimen was controlled within the range of 0.143-0.176 lbs. (65-80 grams), corresponding to an average total thickness of 0.075-inch.

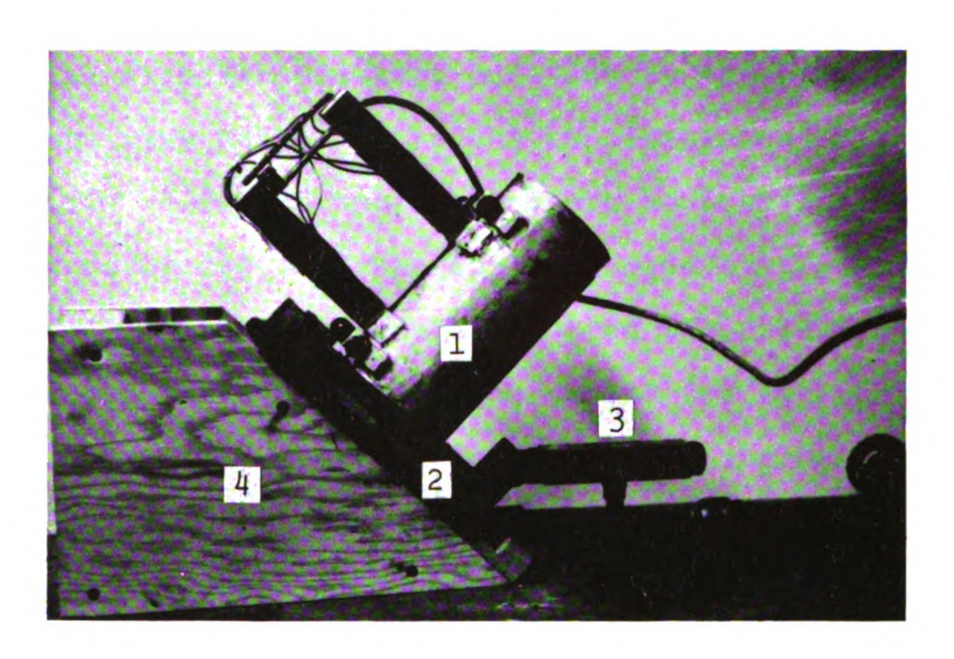
With a small amount of soil in it to prevent the film sticking together, the friction reducer-coated plastic film was applied tightly inside the cylinder. A small cup of soil corresponding to a layer of approximately 1-inch was then put into the cylinder. The pneumatic vibrator vibrated

the cylinder for two minutes for each additional cup of soil. When the soil surface came up near the middle of the cylinder height, the cylinder holder was placed on the 45° holder base so that a 45° surface was created (Fig. 4-5). The lead spheres were placed 1/4-inch apart on this surface by means of an aluminum plate with holes. Then, another cup of soil was added and vibrated. After the cylinder was set in the initial vertical position again, the same process (adding a cup of soil and vibrating for two minutes) was repeated until a desired amount of soil was packed in the cylinder. After covering the top of the packed soil with the upper part of the plastic film, the upper disk plate and the piston rod (total weight is 1.9 lbs.) was put on top of the wrapped soil and the vibration was carried out for three minutes. This completed the preparation of a soil specimen with an average bulk density of 0.0346 lb/in³ (0.96 g/cm^3) , $(\text{range}; 0.0337 - 0.0352 \text{ lb/in}^3)$.

Sometimes a compression test was carried out without a X-ray test, because the transportation to the Veterinary Clinic for X-ray introduced some error in the initial condition of soil. In these cases no lead spheres were needed and the soil was packed just layer after layer without the 45° holder base.

Test Procedure

The compression test was carried out as soon as the soil preparation was finished. Before starting the



- Test cylinder
 Cylinder holder
 Pneumatic vibrator
 Holder base

Fig. 4-5. Packing the Soil in the Cylinder at 45°

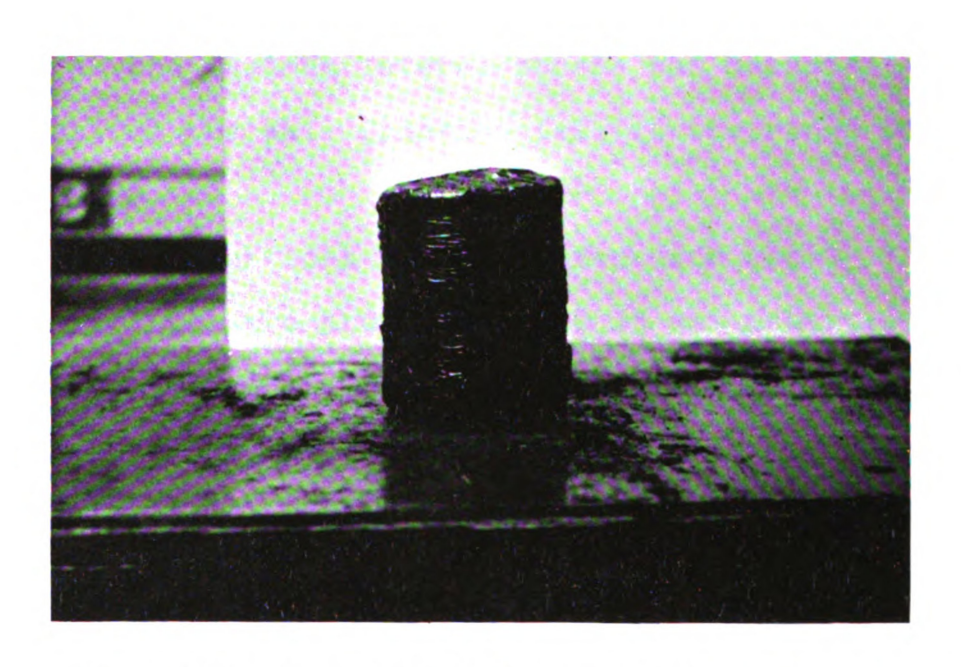


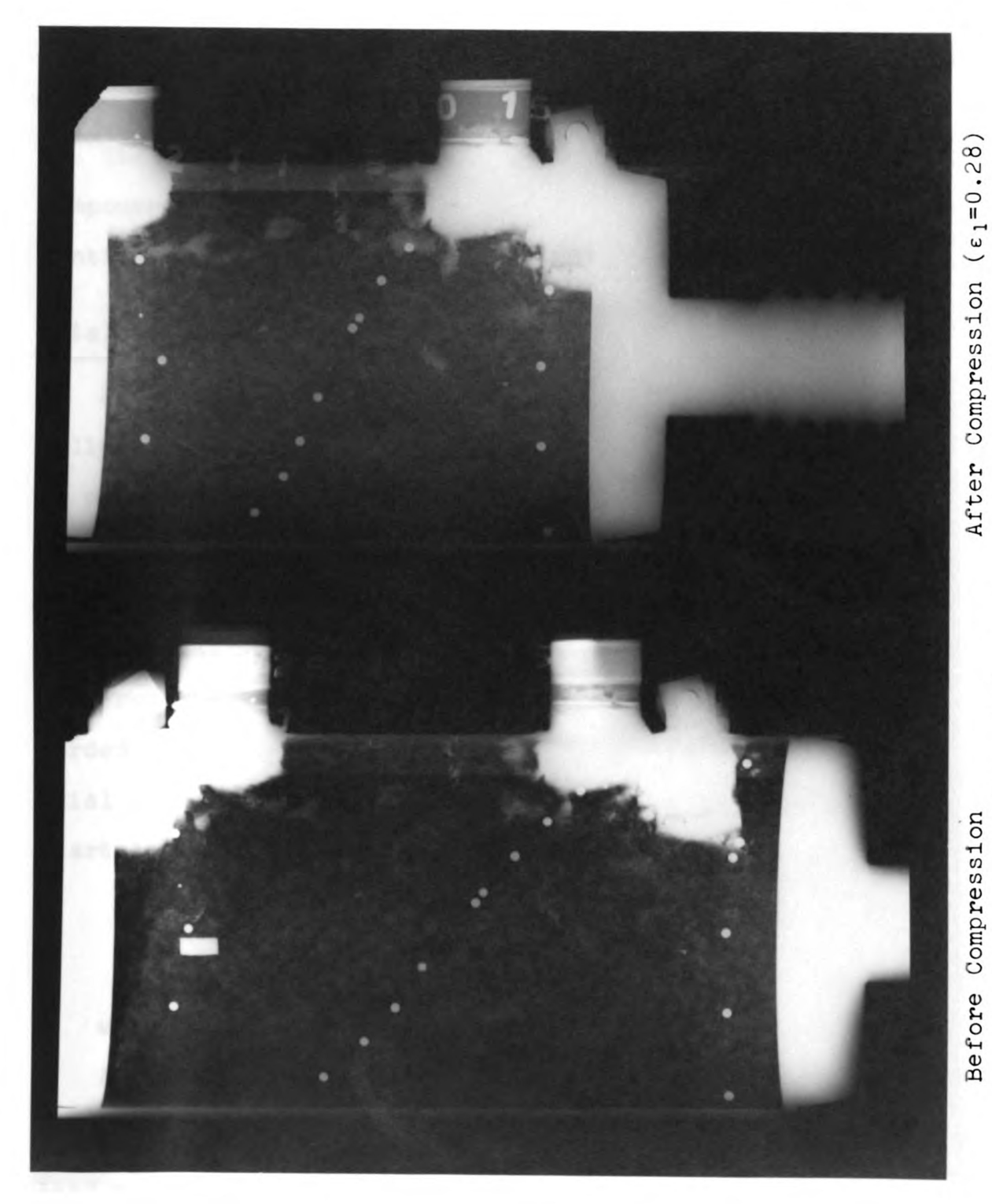
Fig. 4-6. Soil Specimen after Compression (Covered with a thin plastic film sandwitched by the friction reducer)

compression the initial height of the specimen was measured. The initial diameter was kept constant by the holder. The transducers were connected to the amplifiers and the recorders (Fig. 4-4) and the instruments were balanced.

The compression of the soil was made at the rate of 0.092-in/min. The X-Y recorder plotted the axial force versus tangential displacement curve and the strip-chart recorder recorded every separate component versus time. An X-ray picture was taken every 2.5 minutes without stopping the compression and a time mark was put down on the X-Y curve at the time of exposure. The X-ray machine was set for 125 KV, 300mA intensity with 40-inch focal distance and 1.5 second shutter speed. Fig. 4-7 shows two X-ray pictures.

At the end of each test before unloading, the test cylinder was pushed back toward the upper piston and the friction at the maximum lateral stress was measured. The coefficient of the wall friction fell in the range of 0.037 - 0.053.

Three replications were made for each test. Three kinds of springs were chosen so that it was possible to get the stress-strain curves at various levels of lateral confinement. A test with fixed wall $(k \Leftrightarrow \infty)$ was also conducted by replacing the springs and the guide rods with bracing bolts and nuts.



Before Compression Fig. 4-7. X-ray Pictures

V. METHOD OF ANALYSIS

5.1 Stress and Strain Components

The stress components σ_1 , σ_2 and τ , and the strain components ε_1 , ε_2 and γ (natural strain) e_1 , e_2 and γ (conventional strain) are obtained as follows:

Axial Stress o₁

Due to the low friction on the pistons and on the cylinder wall,* the stress distribution in the soil specimen is considered to be uniform. Since the shear stress on the surface of the soil specimen is negligible due to the low friction, the axial and the radial directions are considered as principal directions.

From the axial force transducer output which is recorded on the Y-coordinate of a X-Y recorder chart, the axial force P_1 is obtained by means of the calibration chart App. A-1. Then,

$$\sigma_1 = \frac{P_1}{A}$$

where A is the current area of the soil cylinder, and $A = \pi(r_0 + \Delta r)^2 = \pi r_0^2 (1 + \frac{\Delta r}{r_0})^2 = A_0 (1 + e_2)^2$

^{*} This is also confirmed by the uniform movement of the lead spheres buried near the pistons and the cylinder wall.

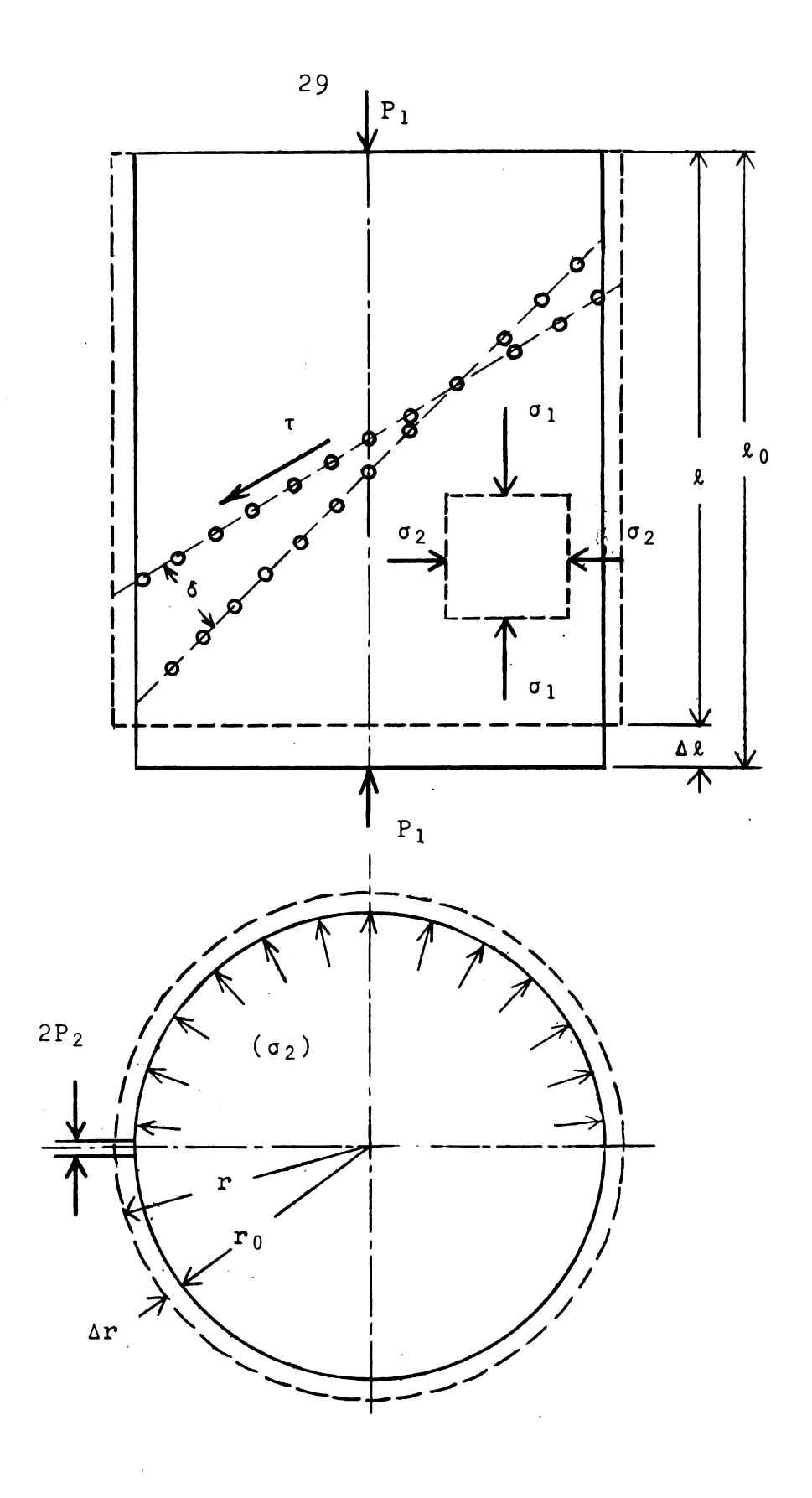


Fig. 5.1. Dimensions of the soil specimen and the stress-strain components.

Therefore,

$$\sigma_1 = \frac{P_1}{A_0(1 + e_2)^2} \tag{5.1}$$

where e_2 is calculated from eq. (5.5).

Axial Strain \textbf{e}_1 and ϵ_1

Since the piston displacement shows complete linearity in terms of compression time t as shown in App. A-2, the axial displacement $\Delta^{\underline{\ell}}$ is obtained from the compression time. Then,

$$e_1 = \frac{\Delta \ell}{\ell 0} \tag{5.2}$$

$$\varepsilon_1 = -\ell_n(1 - e_1) \tag{5.3}$$

This strain is assumed the same for the whole sample for the same reasons given for the axial stress.

Lateral Stress σ_2

The lateral stress is assumed constant along the wall of the cylinder. The equilibrium equation for one-half of the cylindrical shell is considered. The spring force (for one spring = P_2) is in balance with the total force due to σ_2 in the direction of P_2 . Considering the symmetry, the equation of equilibrium becomes

$$2(2P_2) = 2lf^{\frac{\pi}{2}}_{0} (rd\theta)\sigma_2 \sin\theta = 2rl\sigma_2$$

Therefore,

$$\sigma_2 = \frac{2P_2}{rl}$$

Since $P_2 = k\Delta l_2$ where Δl_2 is spring deflection,

$$\sigma_2 = \frac{2k\Delta l_2}{rl} = \frac{2k\Delta l_2}{(r_0 + \Delta r)l}$$

Using the relation $\Delta r = r - r_0 = \frac{2\pi r_0 + \Delta l_2}{2\pi} - r_0 = \frac{\Delta l_2}{2\pi}$,

the above equation becomes

$$\sigma_2 = \frac{4\pi k \Delta r}{(r_0 + \Delta r)\ell} = \frac{4\pi k e_2}{(1 + e_2)(1 - e_1)\ell_0}$$
 (5.4)

where e_1 and e_2 are obtained from eq. (5.2) and eq. (5.5) respectively.

Lateral Strain e_2 and e_2

The lateral strain is also considered to be constant. From Fig. 5-1, eq. (5.5) is obtained. The tangential displacement Δl_2 is obtained from the output records of the lateral displacement transducer by using the calibration chart in App. A-4.

$$e_2 = \frac{\Delta \mathbf{r}}{\mathbf{r}_0} = \frac{\Delta \ell_2}{2\pi \mathbf{r}_0} \tag{5.5}$$

$$\varepsilon_2 = \ln (1 + e_2) \tag{5.6}$$

Shear Stress τ

Since it is assumed that there is no wall friction, both the axial and the radial directions are principal stress directions. The shear stress on the plane of inclination θ from the radial direction is

$$\tau = \frac{\sigma_1 - \sigma_2}{2} \sin 2\theta \tag{5.7}$$

at
$$\theta = \frac{\pi}{4}$$
, $\tau = \frac{\sigma_1 - \sigma_2}{2}$ (5.8)

Shear Strain Y

Shear strain is obtained from the change of the angle of line of lead spheres buried in the soil. As shown in Fig. 5-2,

$$\gamma = 2\delta \tag{5.9}$$

Assuming uniform distribution of the strain, it is also possible to calculate shear strain from the normal strain components in the $\frac{\pi}{4}$ plane as shown in Fig. 5-3.

$$\gamma_{\frac{\pi}{4}} = 2\delta = 2\left[\frac{\pi}{4} - \arctan\left\{\frac{1 - \frac{\Delta \ell}{\ell_0}}{1 + \frac{\Delta r}{r_0}}\right\}\right]$$
 (5.10)

$$\gamma_{\frac{\pi}{4}} \text{ appr.} = \frac{\pi}{2} - 2 \arctan\{1 - e_1 - e_2\}$$

5.2 Mean Normal Stress, Deviatoric Stress and Volume Change

Mean Normal Component and Deviatoric Components

It is common to divide the normal stress into a mean normal component and deviatoric components.

Mean normal component is

$$\sigma_{\rm m} = \frac{\sigma_1 + \sigma_2 + \sigma_3}{3}$$
 in the general case,
$$\sigma_{\rm m} = \frac{\sigma_1 + 2\sigma_2}{3}$$
 for the cylindrical case. (5.11)

Deviatoric components for the cylindrical case are

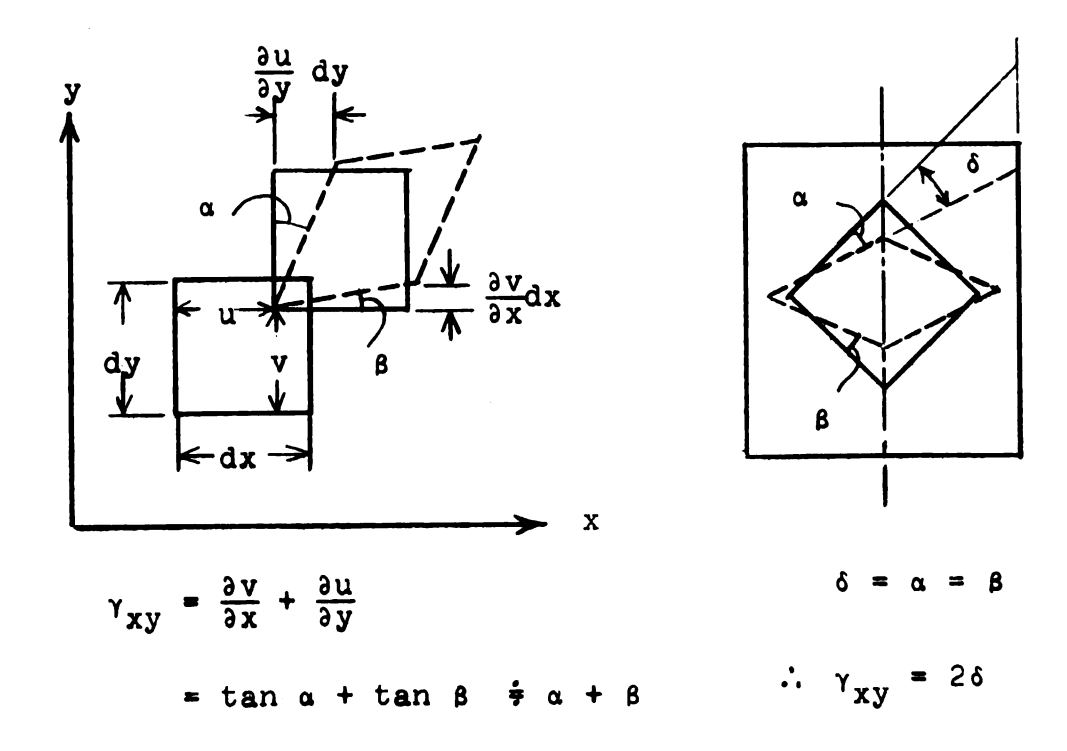


Fig. 5-2. Shear Strain

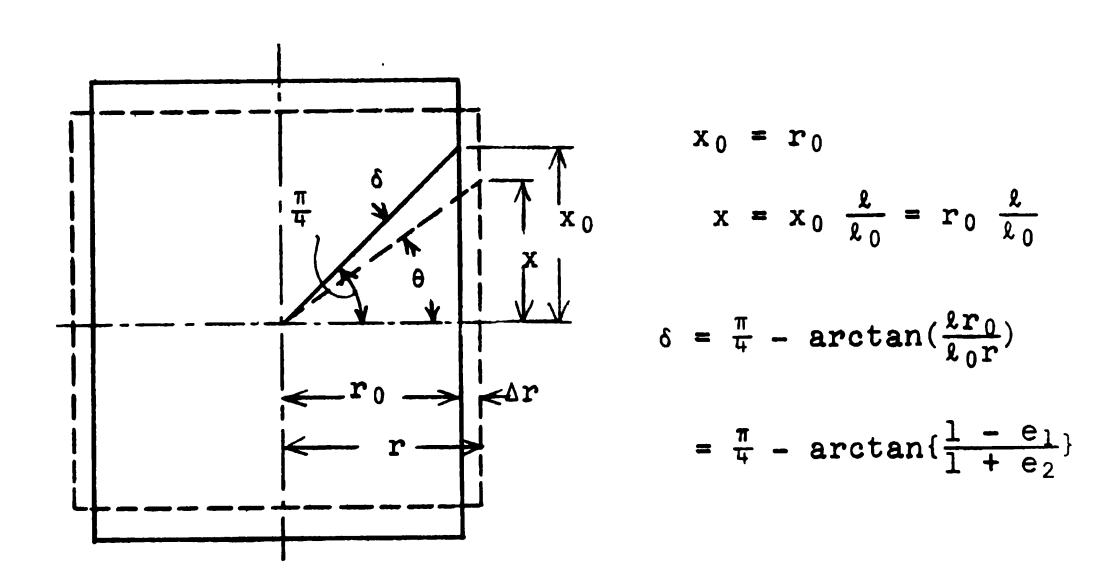


Fig. 5-3. Calculation of $\gamma_{\frac{\pi}{4}}$ from e_1 and e_2

$$\sigma_1' = \sigma_1' - \sigma_m = \frac{2}{3}(\sigma_1 - \sigma_2)$$
 (5.12)

$$\sigma_2' = \sigma_2 - \sigma_m = -\frac{1}{3}(\sigma_1 - \sigma_2)$$
 (5.13)

Deviatoric stress is considered to cause the change of shape. Since both of the components of the deviatoric stress contain $(\sigma_1 - \sigma_2)$, the shear strain γ will be a function of $(\sigma_1 - \sigma_2)$.

$$\gamma = G_1(\sigma_1 - \sigma_2) = G_2(\tau)$$

Volumetric Change

The volumetric change is

$$\frac{\Delta V}{V_0} = \frac{V - V_0}{V_0} = \frac{1}{V_0} \{ 2\pi (\mathbf{r}_0 + \Delta \mathbf{r})^2 (\ell_0 - \Delta \ell) - V_0 \}$$

therefore,

$$\frac{\Delta V}{V_0} = (1 + e_2)^2 (1 - e_1) - 1 \tag{5.14}$$

Eq. (5.14) implies

$$ln(1 + \frac{\Delta V}{V_0}) = 2ln(1 + e_2) + ln(1 - e_1)$$

Therefore,
$$ln(1 + \frac{\Delta V}{V_0}) = 2\epsilon_2 - \epsilon_1$$
 (5.15)

The mean normal stress is generally considered to contribute to the volume change. Therefore, the following function H may be expected.

$$\frac{\Delta V}{V_0} = H(\sigma_m)$$

VI. RESULTS

6.1 Recorded Results

Fig. 6-1 shows the results of 12 tests superimposed on a chart. The three replications for each spring rate show considerable deviation, yet the general tendency due to the change of lateral confinement can be clearly seen. The triangles indicate the same axial displacement (time).

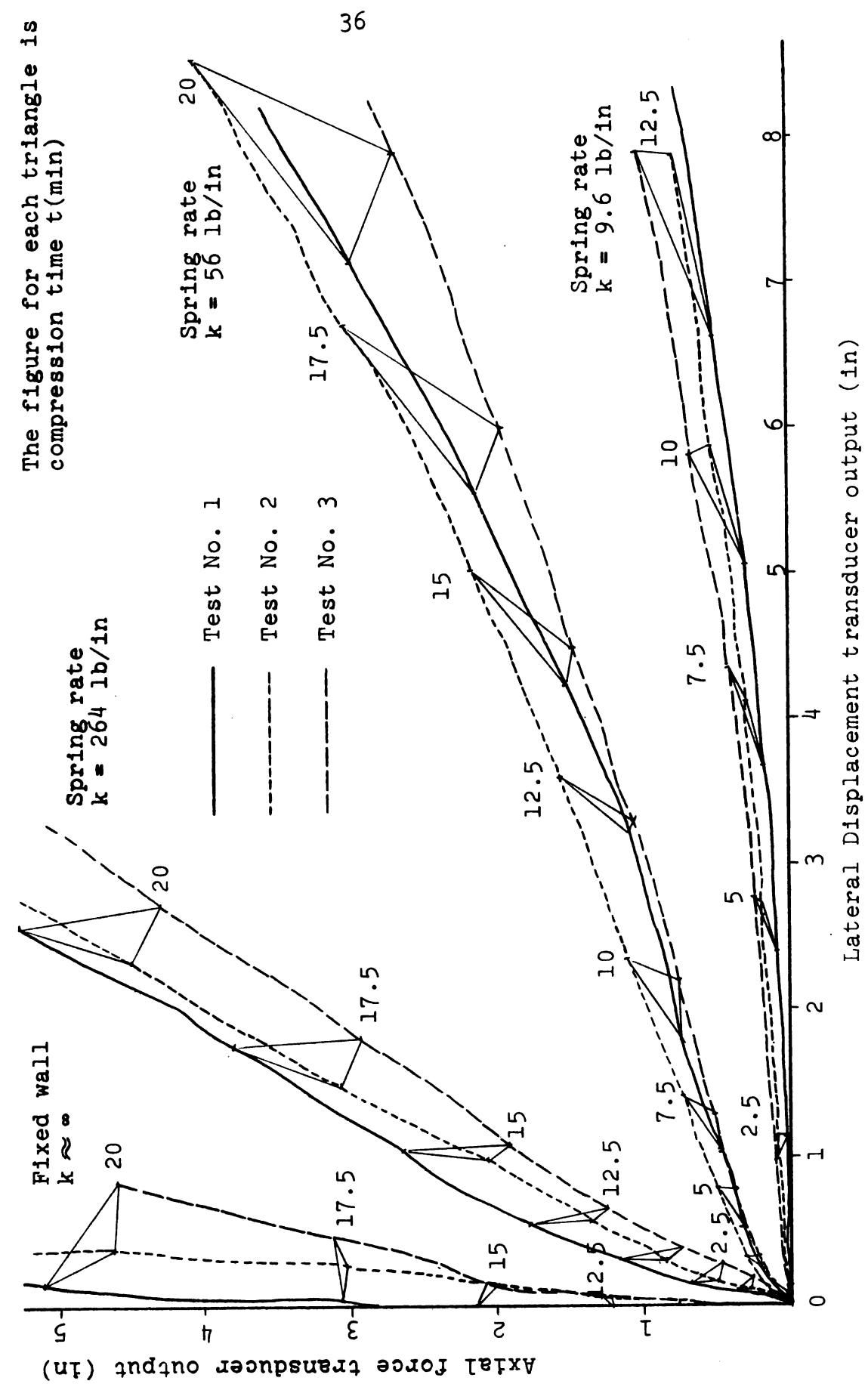
From this record, together with the calibration chart of the transducers in App. A-1, App. A-2 and App. A-4, each component of the stress and strain as well as the volume change was calculated using the equations in Chapter V. The calculated results are tabulated in App. B. The main results are presented graphically in the following sections.

6.2 F_1 and F_2 Functions in Graphs

Fig. 6-2 shows the relationship between σ_1 and ε_2 with ε_1 as contours. Since σ_1 shows a certain unique (single value) functional relationship with ε_1 and ε_2 , a σ_1 value can be obtained graphically if ε_1 and ε_2 values are given.

 σ_2 versus ε_2 and ε_1 relationship is shown in Fig. 6-3. The general tendency is similar to σ_1 versus ε_2 and ε_1 relationship with smaller scale factor for σ_2 . Therefore,





X-Y records for three tests for each of four spring rates Fig. 6-1.

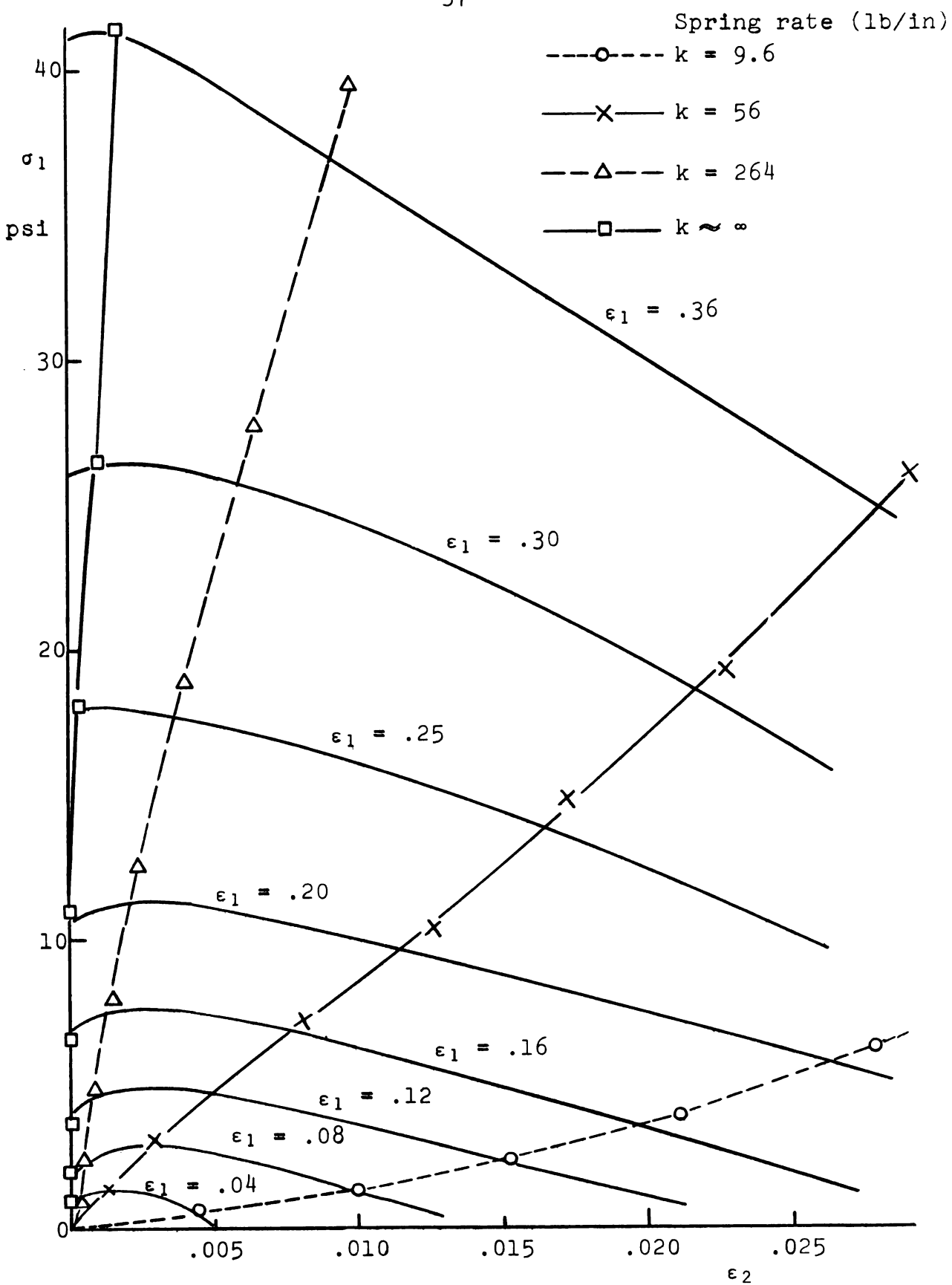


Fig. 6-2. σ_1 versus ε_2 and ε_1 relationship

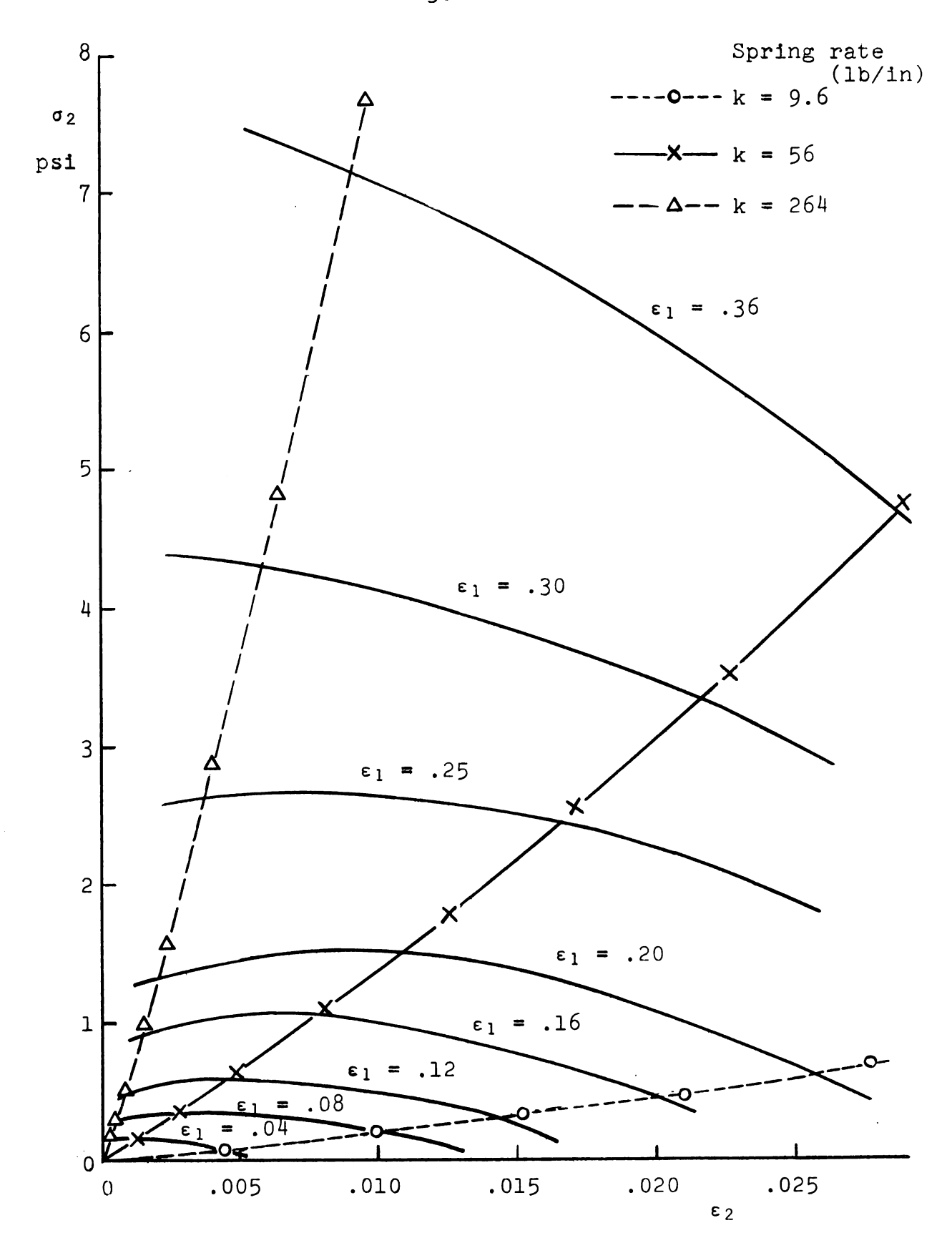


Fig. 6-3. σ_2 versus ε_2 and ε_1 relationship

if ϵ_1 and ϵ_2 are known, σ_2 is directly obtained from this figure. ϵ_1 and ϵ_2 values have to be determined for a practical use of these graphs. This can be done by X-ray method burying lead spheres in the soil at every node of an imaginary network.

Since formulation of F_1 and F_2 introduces a certain error, this graphical method may be the most accurate way to get the stress components if the ϵ_1 and ϵ_2 network is dense enough.

6.3 σ_1 versus ε_1 Relationship

Fig. 6-4 shows the relationship between σ_1 and ε_1 . In the higher compression range the effect of spring rate is clear: higher spring rate creates higher axial stress at the same level of axial strain. In the lower compression range, the effect of spring rate is, however, inconsistent. This may partly come from the variation of initial density ranging from 0.0337 to 0.0352 lb/in³. This variation corresponds to a variation in axial displacement amounting up to 0.26-inch (ε_1 = 0.044) which is large enough to create the inconsistency. The low initial density might be another reason, because in lower density, soil particles and aggregates have more freedom of sliding or rolling. This might imply a more unstable mechanical condition which makes it possible for the soil to take more than one stress path in the compression process.

The smaller slope of the initial compression lines of $\log \sigma_1$ versus $\log \varepsilon_F$ curves in Fig. 6-5 indicates that

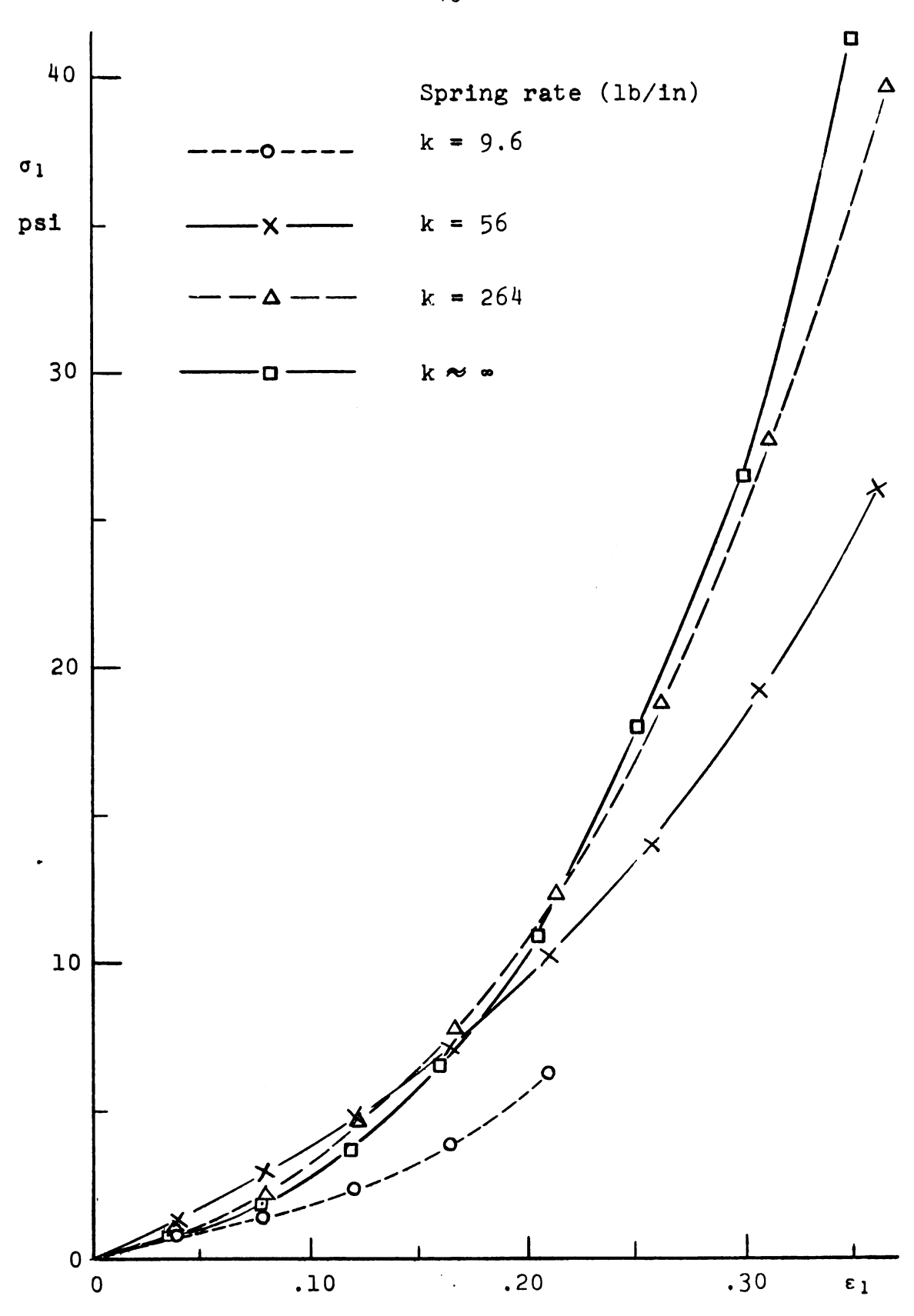


Fig. 6-4. σ_1 versus ε_1 relationship

there may be some critical point where the soil becomes more stable and begins to show a higher rate of work-hardening.

There are two commonly used soil compression equations which may fit to the test results. They are a modified form of Bekker's sinkage equation and of the consolidation equation (eq.(2.4) and eq.(2.6)). Fig. 6-5 shows log σ_1 versus $\log \varepsilon_1$ relationship, where eq. (2.6) should be a straight line. Fig. 6-6 presents $\log \sigma_1$ versus ε_1 relationship, where eq. (2.4) should be a straight line. The $\log \sigma_1$ versus ε_1 curves in Fig. 6-6 are not linear. This means that the equation similar to the consolidation equation is not valid here. The $\log \sigma_1$ versus $\log \varepsilon_1$ relation in Fig. 6-5 can be represented by two straight lines which are described by the following equation with different values for the constants a and n.

$$\sigma_1 = a \varepsilon_1^n$$
 (6.1)

This means that the equation similar to Bekker's sinkage equation is valid.

6.4 σ_1 versus σ_2 Relationship

The relationship between σ_1 and σ_2 is shown in Fig. 6-7. From this figure, there seems to exist a linear relationship between σ_1 and σ_2 that can be expressed by

$$\sigma_2 = \mu \sigma_1. \tag{6.2}$$

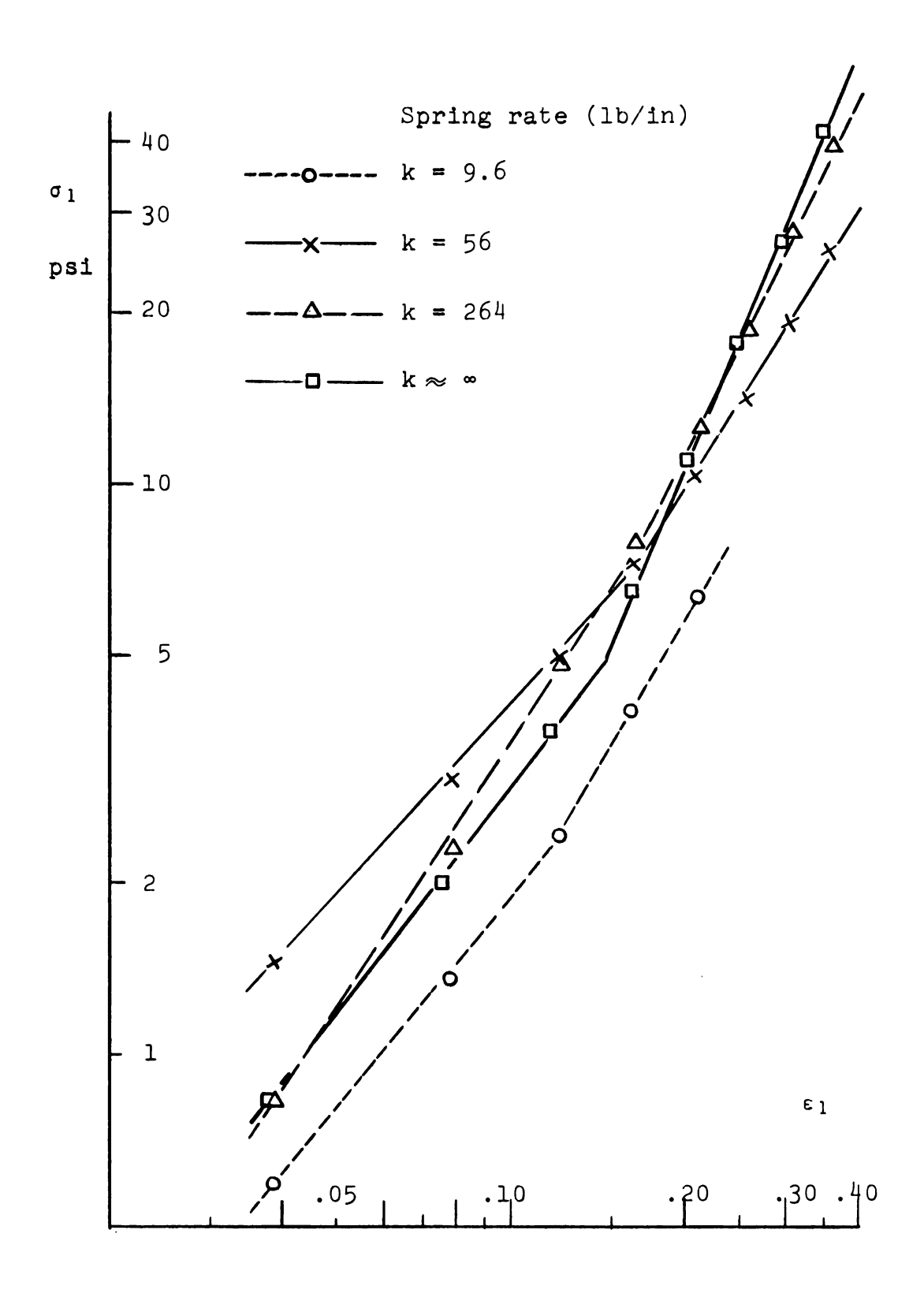


Fig. 6-5. $\log \sigma_1$ versus $\log \varepsilon_1$ lines



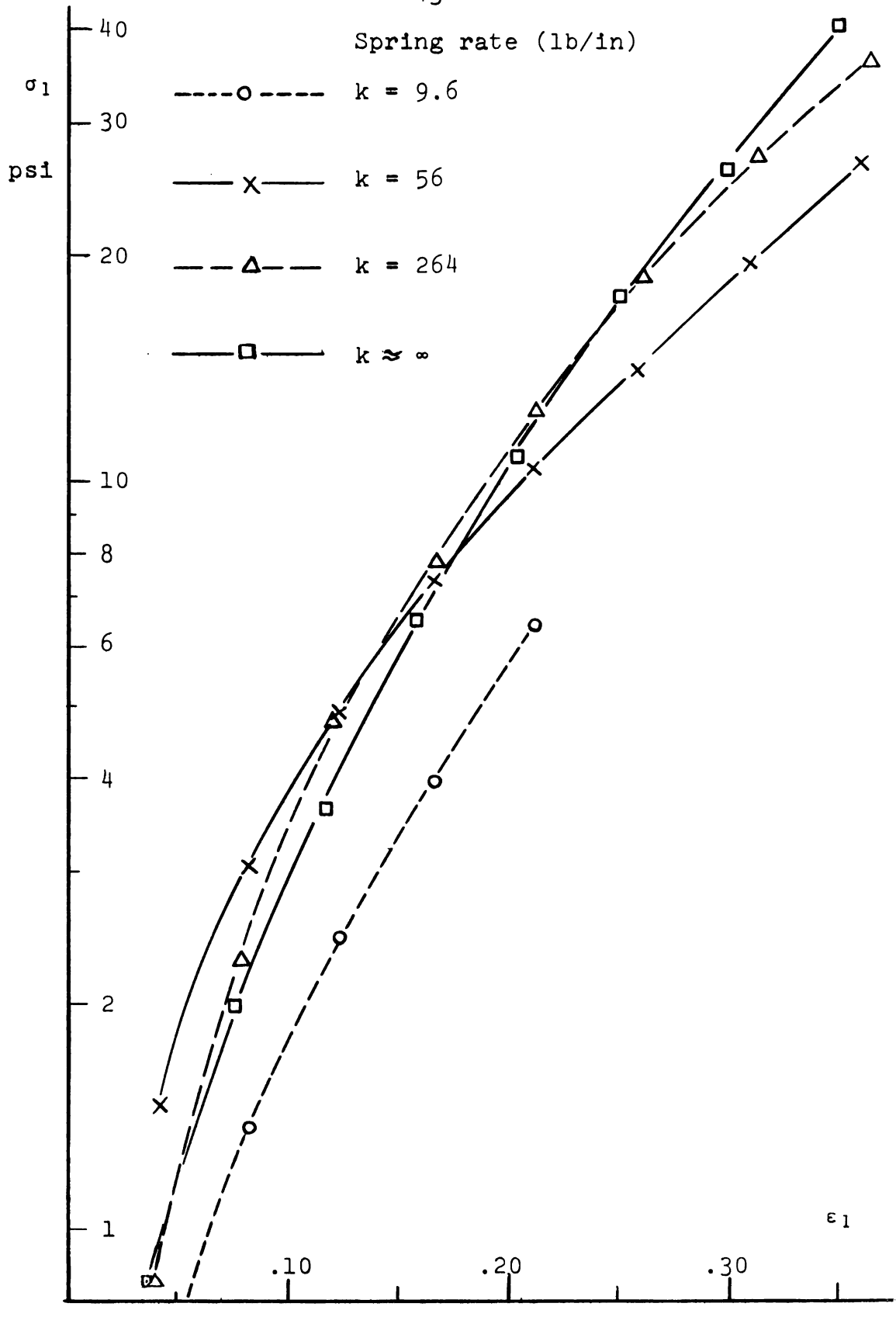


Fig. 6-6. $\log \sigma_1$ versus ϵ_1 curves

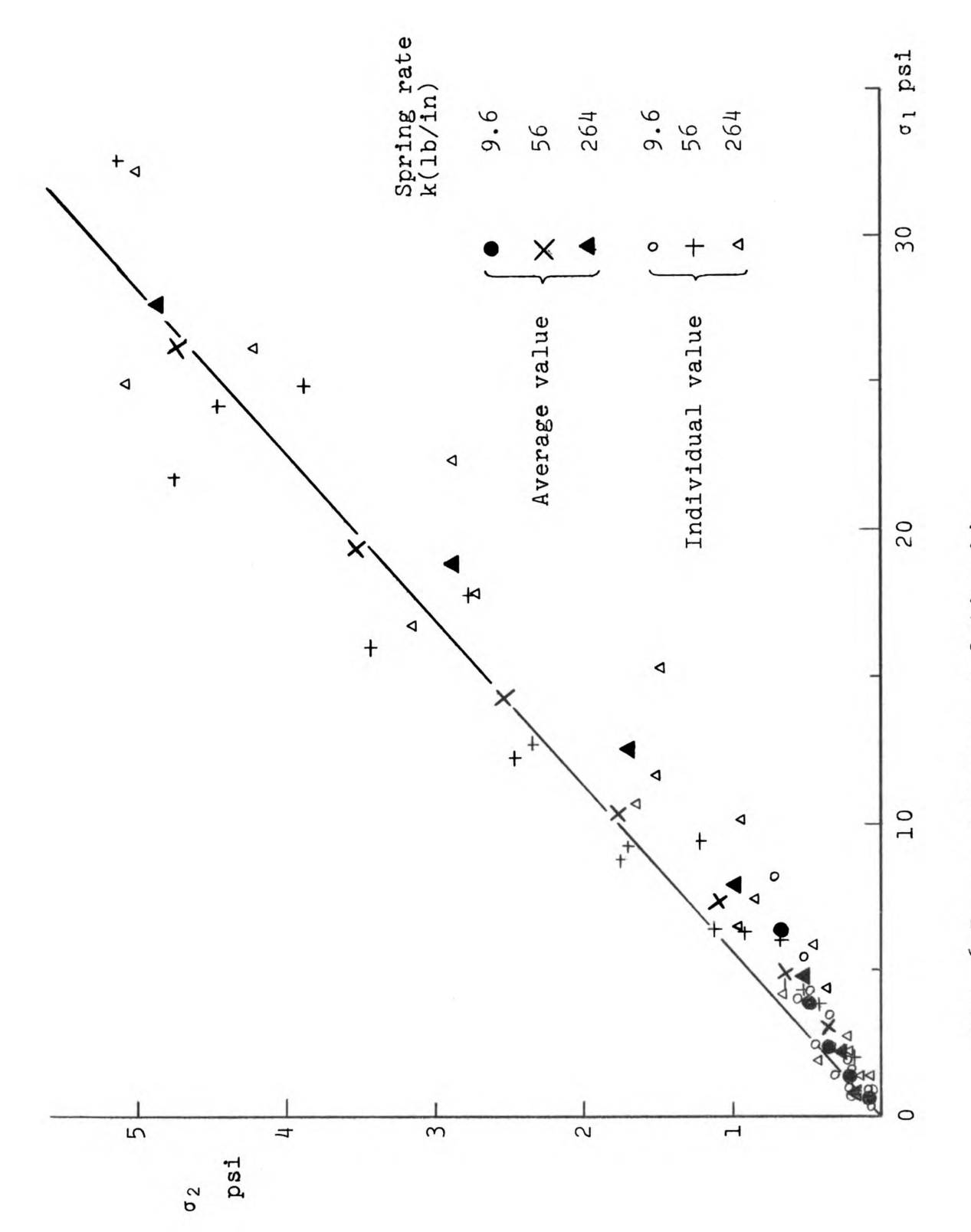


Fig. 6-7. o₁ versus o₂ relationship

The μ values which are calculated from App. B-1 and App. B-3 are tabulated in Table 6-1.

TABLE 6-1.-- $\mu = \sigma_2/\sigma_1$ values.

Axial	displacement Δl(in)	S	Spring rate k(lb/in)	
		k = 9.6	k = 56	k = 264
	0.23	0.151	0.108	0.202
	0.46	0.156	0.115	0.130
	0.69	0.139	0.130	0.103
	0.92	0.122	0.152	0.123
	1.15	0.105	0.172	0.125
	1.38		0.179	0.152
	1.61		0.181	0.174
	1.84		0.181	0.194

Considering the large variation of μ values calculated for the individual test (App. B-9), it will be possible to assume that μ is a constant for various lateral strain confinement within this test range of ϵ_1 < .36 and ϵ_2 < .029 and with a possible exception for the very low compression range. The idea of μ = constant is similar to the idea of the coefficient of earth pressure in soil mechanics. The coefficient of earth pressure is defined as the ratio of the lateral stress to the vertical stress. According to Scott (1963) p. 403, this coefficient is defined for both the soil conditions at failure and below failure (soil at

rest). The earth pressure coefficient is considered as a constant for a soil of semi-infinite mass in which a soil element under a vertical pressure can expand laterally with certain lateral confinement, which is similar situation to this test. The average value of μ here in this test is $\mu = 0.141$.

6.5 τ versus γ Relationship

The γ values measured from X-ray pictures show good coincidence with γ calculated from e_1 and e_2 (eq. (5.10)) as shown in Fig. 6-8. This fact implies that the effect of the wall friction is small. Since the latter calculation method has higher accuracy so far as the wall friction is negligible, the values calculated from e_1 and e_2 are used for the following discussion. The τ values were calculated from σ_1 and σ_2 using eq. (5.8).

Fig. 6-9 shows the relationship between τ and γ . Spring rate apparently affect the τ value. This indicates that τ is not a function of γ alone.

6.6
$$\sigma_{m}$$
 versus $\frac{\Delta V}{V_{0}}$ Relationship

Fig. 6-10 gives the relationship between the mean normal stress and the volume change. The figure shows approximately the same tendency for all spring rates.

The σ_m versus $\frac{\Delta V}{V_0}$ relationship on a log-log chart is shown in Fig. 6-11. The same relationship is shown on a semi-log chart in Fig. 6-12.

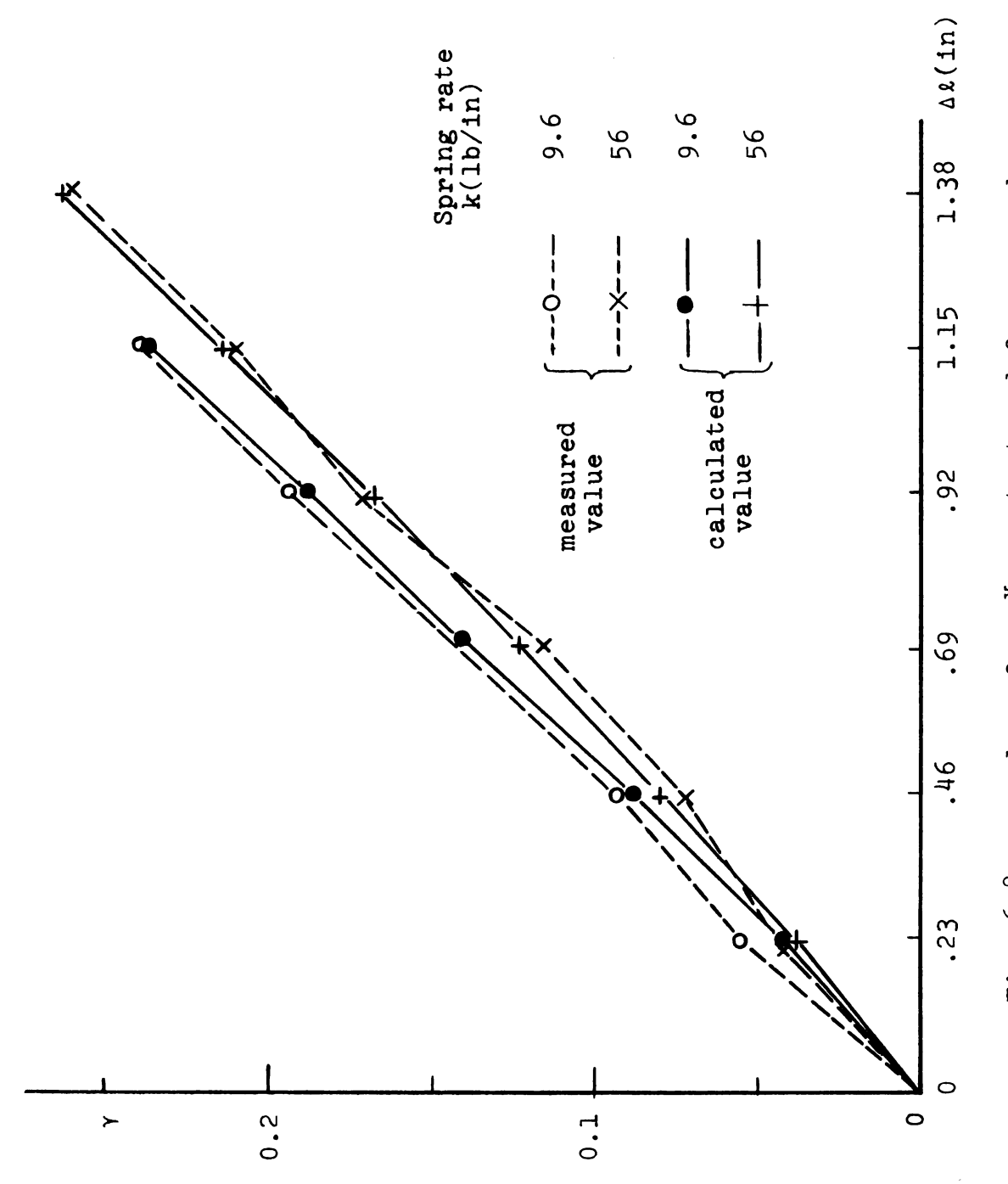


Fig. 6-8. γ values from X-ray test and from e₁ and e₂



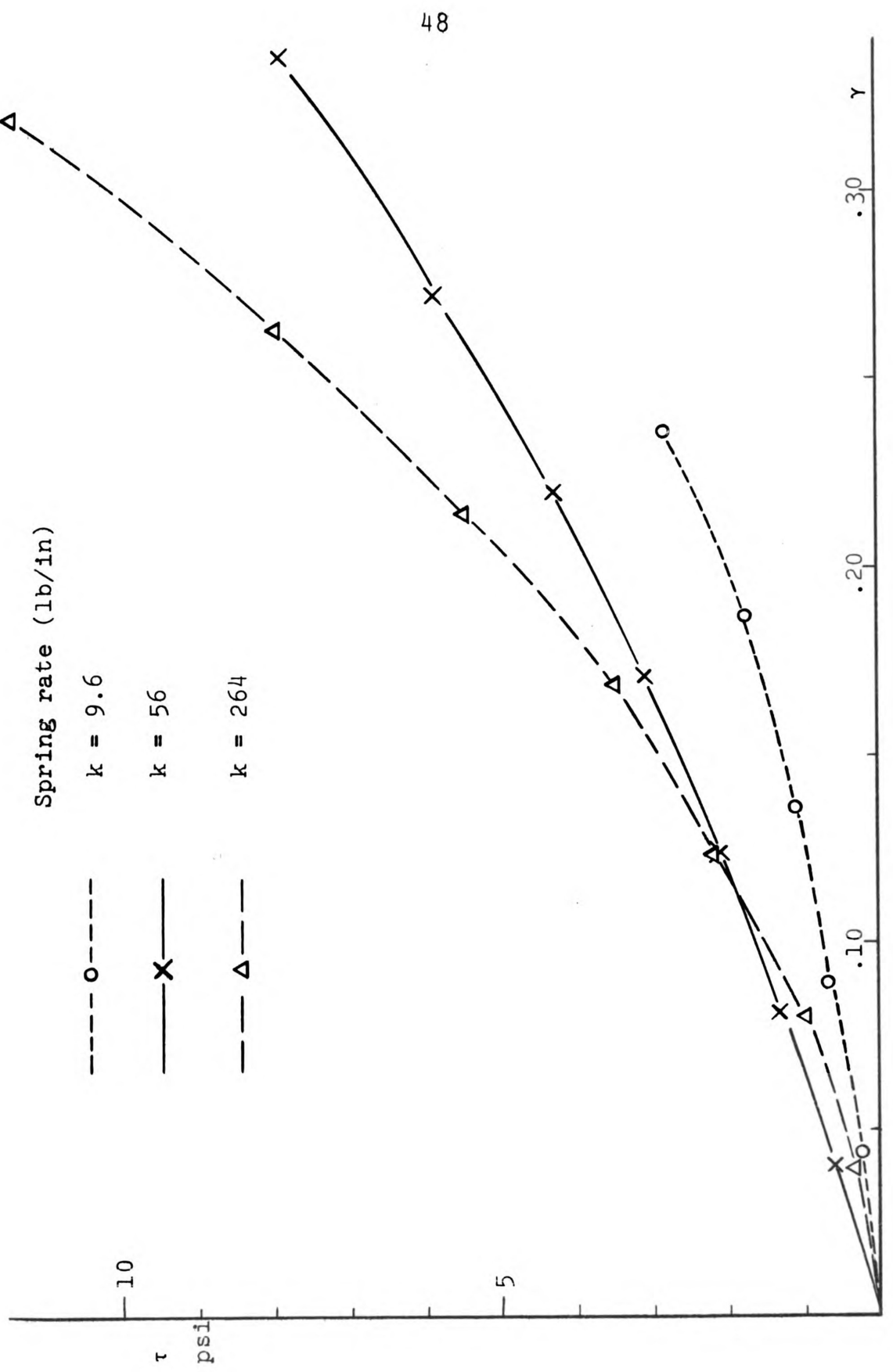


Fig. 6-9. τ versus γ relationship

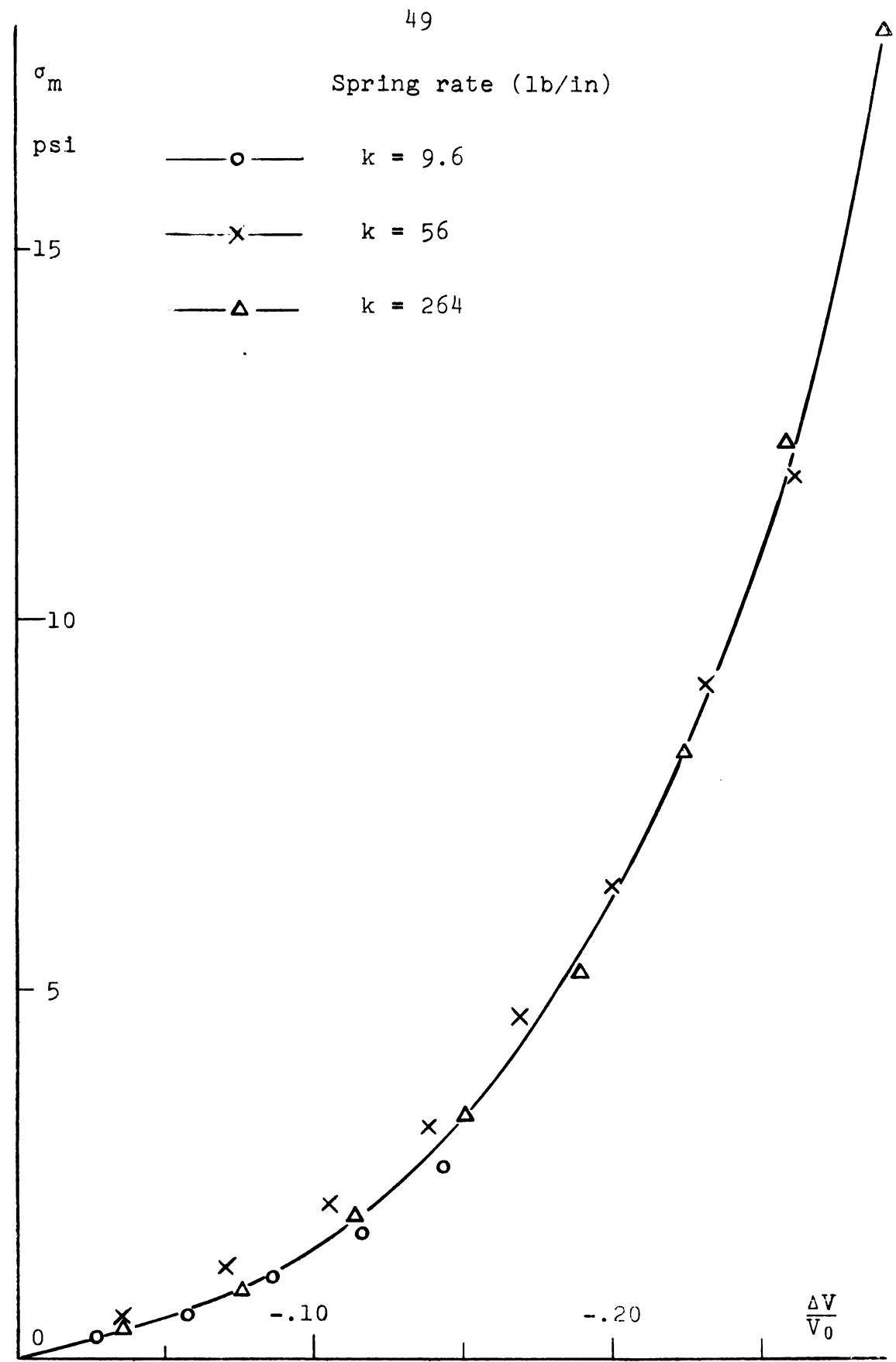


Fig. 6-10. σ_{m} versus $\Delta V/V_{0}$ relationship

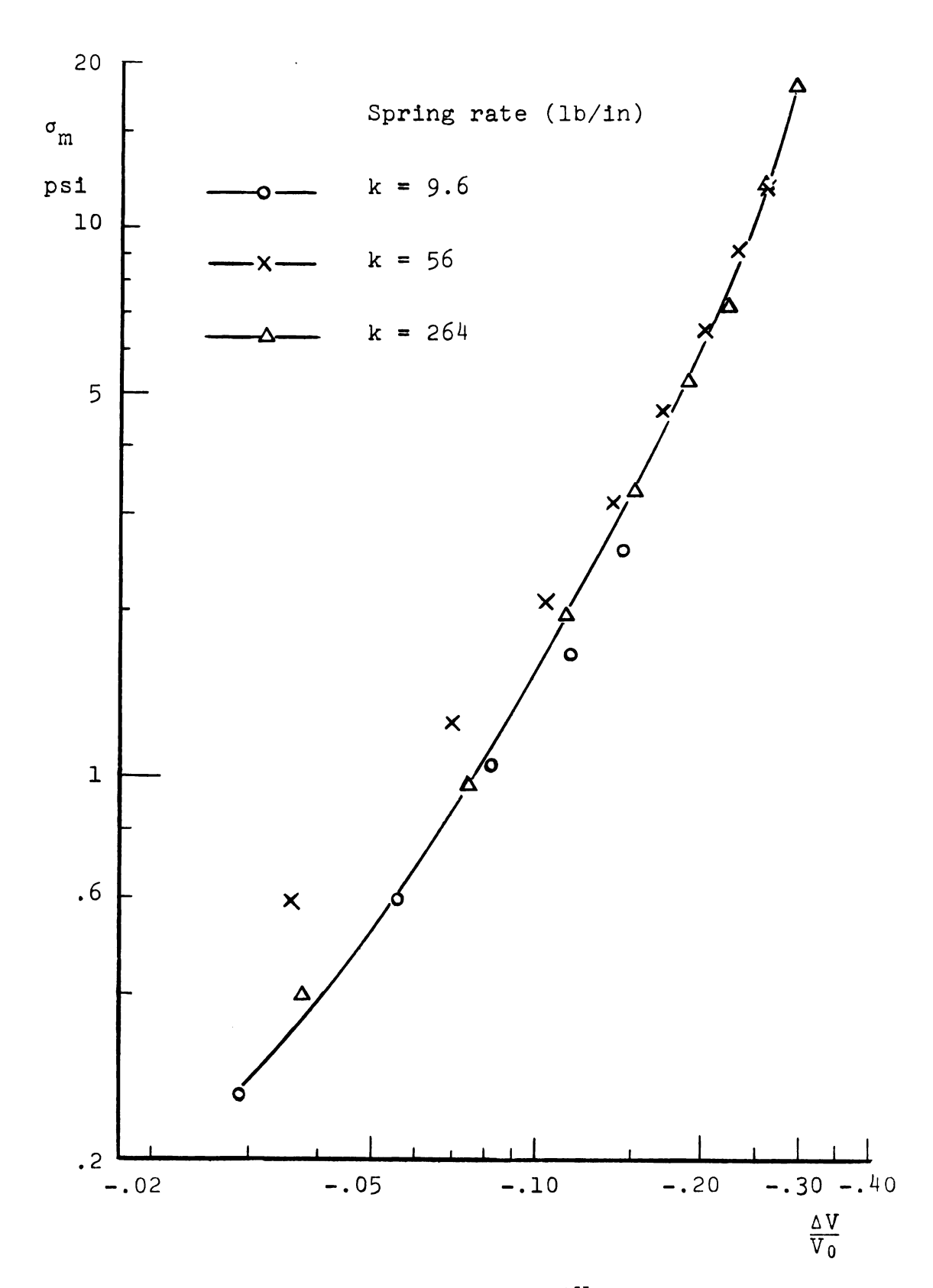


Fig. 6-11.--log $\boldsymbol{\sigma}_m$ versus log $\frac{\Delta \, V}{V_0}$ relationship.

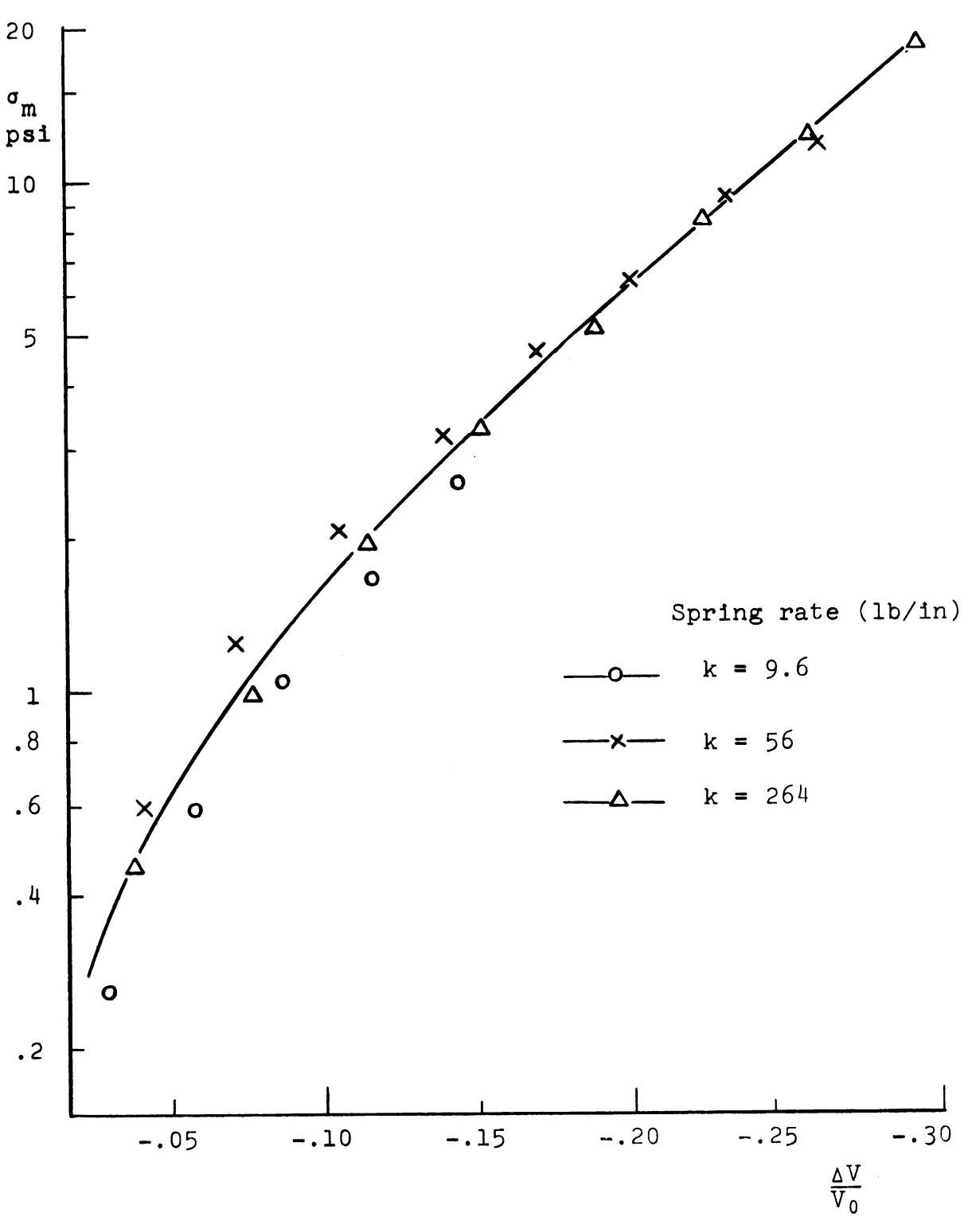


Fig. 6-12.--log σ_m versus $\frac{\Delta \, V}{V_0}$ relationship.

Fig. 6-12 shows approximately a straight line in the higher compression range of $\epsilon_1 > 0.15$. This straight line is expressed by eq. (6.3).

$$\log \sigma_{m} = k_{0} \cdot \frac{\Delta V}{V_{0}} \qquad \text{for } \epsilon_{1} > 0.15$$
 (6.13)

where k_0 is a constant.

This is a similar form to the original consolidation equation.

Since τ takes various values at the same level of γ and τ is linearly related to σ_m as discussed later in Chapter VII. 7.2, the bulk density (or volume) calculated from Vanden-Berg's equation (2.7) will take various values for the same value of σ_m . This conflicts with the fact that σ_m versus $\frac{\Delta V}{V_0}$ curve shows approximately the same tendency for various lateral confinements. VandenBerg's equation does not, therefore, seem to be valid here.

VII. DISCUSSION

7.1 Strain-hardening Theory and F_1 and F_2 Functions

The principal stress components σ_1 and σ_2 are obtained graphically from Fig. 6-2 and Fig. 6-3 if two principal strain components ε_1 and ε_2 are known. This is, however, not suitable for calculations of a general case. For the development of a general theory, the F_1 and F_2 functions have to be formulated.

Isotropic Hardening Formula

The theory of strain-hardening developed in metal plasticity may be useful to explain the increase in soil strength with compaction and to formulate a stress-strain relationship for soil. The basic idea of isotropic hardening theory is quoted from Hill (1950) p. 23.

Assuming that a material is work-hardened isotropically, the one-dimensional stress-strain relationship $\sigma_{x} = \mathrm{H}_{I}(\varepsilon_{px}) \text{ (p implies plastic component of strain) can be extended to the two- or three-dimensional case by using a generalized stress <math>\overline{\sigma}$ and a generalized strain $\overline{\varepsilon}_{p}$. The one-dimensional relationship can be easily obtained from a tensile test of a metal piece for example, and the

function form $H_{\overline{I}}$ is determined. Then, the same function $H_{\overline{I}}$ can be assumed for $\overline{\sigma}$ and $\int\!d\,\overline{\epsilon}_{D}^{}.$

$$\bar{\sigma} = H_{I}(\int d\bar{\epsilon}_{p})$$
 (7.1)

Since a soft surface soil has only negligible elastic strain, it can be assumed that the total strain* equals plastic strain for soil, that is, $\overline{\epsilon}_p = \overline{\epsilon}$. It is also assumed here that $\int d\overline{\epsilon} = \overline{\epsilon}$. Thus eq. (7.1) becomes

$$\overline{\sigma} = H_T(\overline{\varepsilon})$$
 (7.2)

where
$$\bar{\sigma} = \sqrt{\frac{3}{2}\sigma_{ij}^{\dagger}\sigma_{ij}^{\dagger}}$$
 (7.3)

$$\overline{\varepsilon} = \sqrt{\frac{2}{3}\varepsilon_{ij}} \varepsilon_{ij}$$
 (7.4)

For the cylindrical case,

$$\sigma_{1}' = \frac{2(\sigma_{1} - \sigma_{2})}{3}$$
 and $\sigma_{2}' = \sigma_{3}' = -\frac{(\sigma_{1} - \sigma_{2})}{3}$

Therefore,

$$\overline{\sigma} = \sqrt{\frac{3}{2}(\sigma_1 - \sigma_2)^2 \{(\frac{2}{3})^2 + (-\frac{1}{3})^2 + (-\frac{1}{3})^2\}} = \sigma_1 - \sigma_2$$

$$\overline{\varepsilon} = \sqrt{\frac{2}{3}(\varepsilon_1^2 + 2\varepsilon_2^2)}$$
(7.5)

The soil test corresponding to the tensile test of metals will be a compression test without lateral confinement. It is, however, almost impossible to do this test for a soft soil. Instead, the necessary relationship can be

^{*}Total strain includes volumetric strain, because it contributes to the strain-hardening.

obtained from a compression test of soil in a fixed wall cylinder with suitable friction reducer on the wall. In this case σ_2 is no longer zero. Extending the test result of eq. (6-2) to the fixed wall case, σ_2 can be calculated from $\sigma_2 = \mu \sigma_1$. And, for this case $\sigma_1 - \sigma_2 = \overline{\sigma}$ and $\varepsilon_1 = \sqrt{\frac{3}{2}} \, \overline{\varepsilon}$ (as a special case of eq. (7.5)).

From the fixed wall test result presented in Chapter VI. 6.3, the same equation as eq. (6.1) can be used for ${\rm H}_{\rm I}$ function.

$$\sigma_1 = a\varepsilon_1^n$$
 for $\varepsilon_1 > 0.15$ (7.6)
where $a = 493$ (psi)
 $n = 2.414$

Since in the lower compression range of $\epsilon_1 \leq 0.15$, the effect of lateral confinement is not consistent as discussed in Chapter VI. 6.3, the theoretical consideration here is limited to the higher compression range of $\epsilon_1 > 0.15$.

Since eq. (7.6) is introduced, the prototype equation becomes

$$\sigma_1 - \sigma_2 = (1 - \mu)a\epsilon_1^n \qquad (7.7)$$

Therefore the general form is

$$\overline{\sigma} = (1 - \mu)a(\sqrt{\frac{3}{2}} \overline{\epsilon})^n$$
 (7.8)

Substituting eq. (7.5) into eq. (7.8),

$$\sigma_1 - \sigma_2 = (1 - \mu)a\{\sqrt{\frac{3}{2}} \cdot \sqrt{\frac{2}{3}(\epsilon_1^2 + 2\epsilon_2^2)}\}^n$$

and using eq. (6.2), eq. (7.9) is obtained.

$$\sigma_1 = \mathbf{a}(\varepsilon_1^2 + 2\varepsilon_2^2)^{\frac{n}{2}} \tag{7.9}$$

However, this formula looks unreasonable because σ_1 increases as ϵ_2 increases even if ϵ_2 is in the direction of expansion. Strain-hardening of metals occurs equally under compression or tension. For soils, the situation is different, soil is work-hardened by compression but softened by expansion. Therefore, the plus sign in front of $2\epsilon_2^2$ could be changed into a minus sign in the case of expansion. If ϵ_2 is in the direction of compression the sign should remain plus. Then, the following equations are obtained.

$$\sigma_1 = a(\varepsilon_1^2 - 2\varepsilon_2^2)^{\frac{n}{2}}$$
 (7.10)

$$\sigma_2 = \mu a(\varepsilon_1^2 - 2\varepsilon_2^2)^{\frac{n}{2}}$$
 (7.11)

The σ_1 values calculated from eq. (7.10) are listed in App. C-1. The comparison between the calculated values and the measured values is shown in Fig. 7-1. It shows almost no effect of ε_2 . It also shows a large deviation from the measured value when the lateral confinement is weak. This might mainly be due to the fact that in soil only a small strain is produced in the lateral direction even if a large axial strain is put in; in other words, $\varepsilon_2/\varepsilon_1$ values for soils are comparatively smaller than for metals.

Fig. 7-1. σ_1 from Isotropic hardening theory.

The reason will be that most of the input energy is dissipated in the form of volume change and only a small part is used for lateral expansion. Probably soil is not workhardened isotropically as is metal.

Modification of Isotropic Hardening Equation

1. One of the main reasons for the discrepancy of eq. (7.10) with the test results will be the assumption that ε_1 and ε_2 contribute equally to σ_1 . If it is assumed that a part of σ_1 is contributed from σ_2 (that is, $\sigma_1 = \sigma_1(1) + \sigma_1(2)$) and also $\sigma_2 = a\varepsilon_2^n$ as well as $\sigma_2 = \mu\sigma_1$, then $\sigma_1(1) = a\varepsilon_1^n$ and $\sigma_1(2) = -\frac{1}{\mu}a\varepsilon_2^n$. Also modifying eq. (7.10) into a simpler form, eq. (7.12) is obtained.

$$\sigma_1 = a(\varepsilon_1^n - \frac{1}{u} \varepsilon_2^n)$$
 (7.12)

However eq. (7.12) has the same tendency as eq. (7.10) as shown in Fig. 7-2 and App. C-2.

2. The discrepancy of eq. (7.12) mainly comes from the assumption $\sigma_2 = a\varepsilon_2^n$ based upon some idea of isotropy. This assumption together with $\sigma_2 = \mu\sigma_1$ leads us to the relationship $\frac{\varepsilon_2^n}{\varepsilon_1^{n}} = \mu$. The test result apparently shows that this ratio is not a constant. That means there is a nonlinear interaction between ε_1 and ε_2 . This may be described in the form of $\sigma_1 = f_1(\varepsilon_1) + f_2(\varepsilon_2) + f_3(\varepsilon_1, \varepsilon_2)$. If the interaction $f_3(\varepsilon_1, \varepsilon_2)$ is expressed by a form of polynomial $\sum_{i=1}^{n-1} b_i \varepsilon_1^{n-i} (n2\varepsilon_2)^i$, then it may be reasonable to modify eq. i=1

Fig. 7-2. σ_1 from the modified equation (1).

 ϵ_1

$$\sigma_1 = a\{\epsilon_1 - n(2\epsilon_2)\}^n \tag{7.13}$$

where η is a contribution factor of ϵ_2 to ϵ_1 .

If the contribution factor $\eta=1$, that is, the interaction term is contributed equally from ϵ_1 and ϵ_2 , the following form is derived.

$$\sigma_1 = a(\varepsilon_1 - 2\varepsilon_2)^n \tag{7.14}$$

The calculated value of σ_1 according to eq. (7.14) is given in Fig. 7-3 and App. C-3. The same a and n values from the fixed wall test as in the calculation of eq. (7.10) were used for this calculation. The calculated results show fairly good agreement with the test results for various lateral confinements.

Using the equation $\sigma_2 = \mu \sigma_1$, eq. (7.15) is obtained.

$$\sigma_2 = \mu a(\varepsilon_1 - 2\varepsilon_2)^n \tag{7.15}$$

The calculated values of σ_2 from eq. (7.15) are given in Fig. 7-4 and App. C-4. Considering the fairly large variation in μ value, the calculated values are considered to be approximately in agreement with the measured values.

Since $(\sigma_1 - \sigma_2)$ is the generalized stress in the cylindrical case, the general form corresponding to eq. (7.8) is $\sigma_1 - \sigma_2 = (1 - \mu)a(\varepsilon_1 - 2\varepsilon_2)^n$ (7.16) log $(\sigma_1 - \sigma_2)$ versus log $(\varepsilon_1 - 2\varepsilon_2)$ relationship should be a straight line. This is shown in Fig. 7-5 in which measured values are plotted.

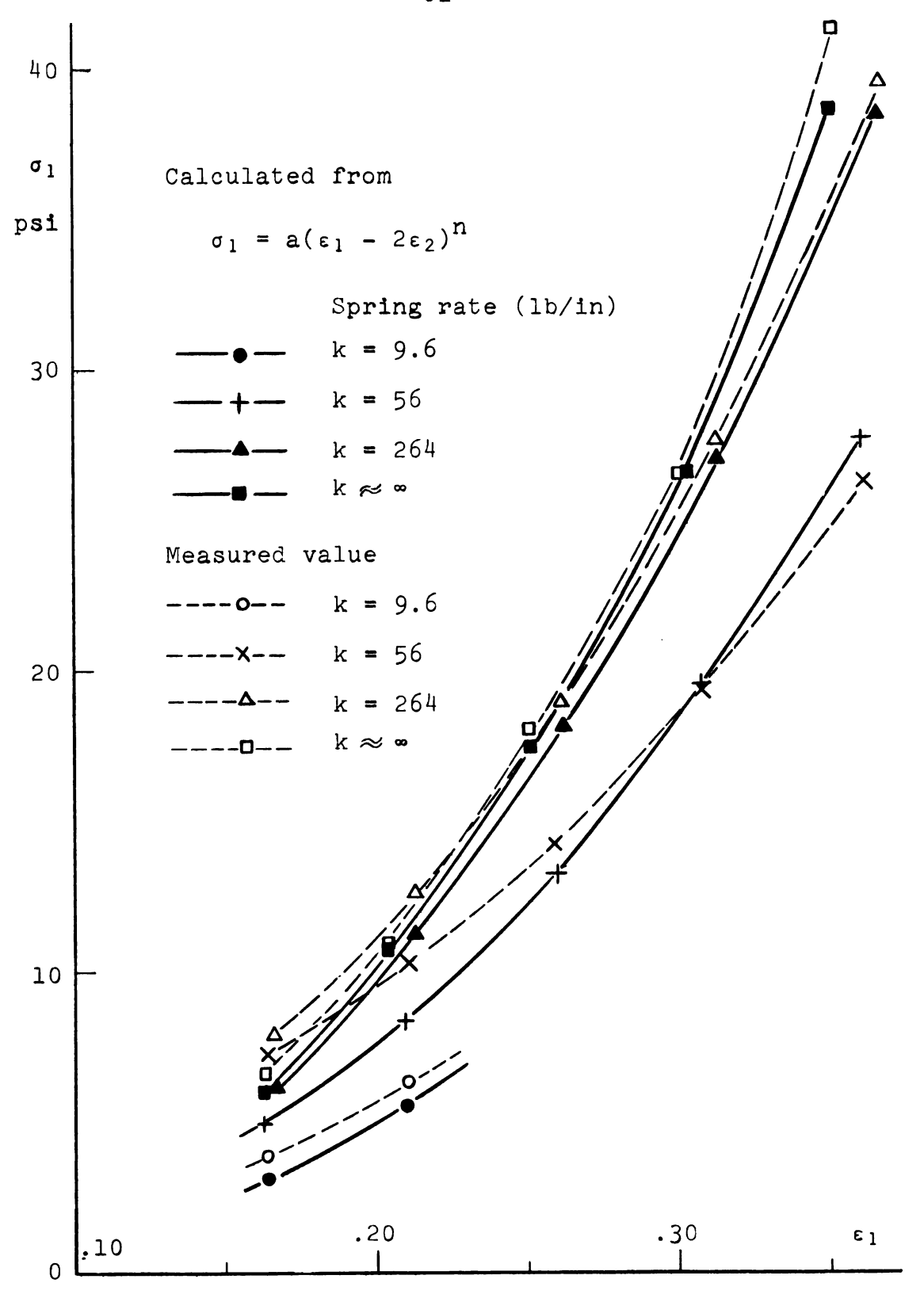


Fig. 7-3. σ_1 from the modified equation (2) η = 1

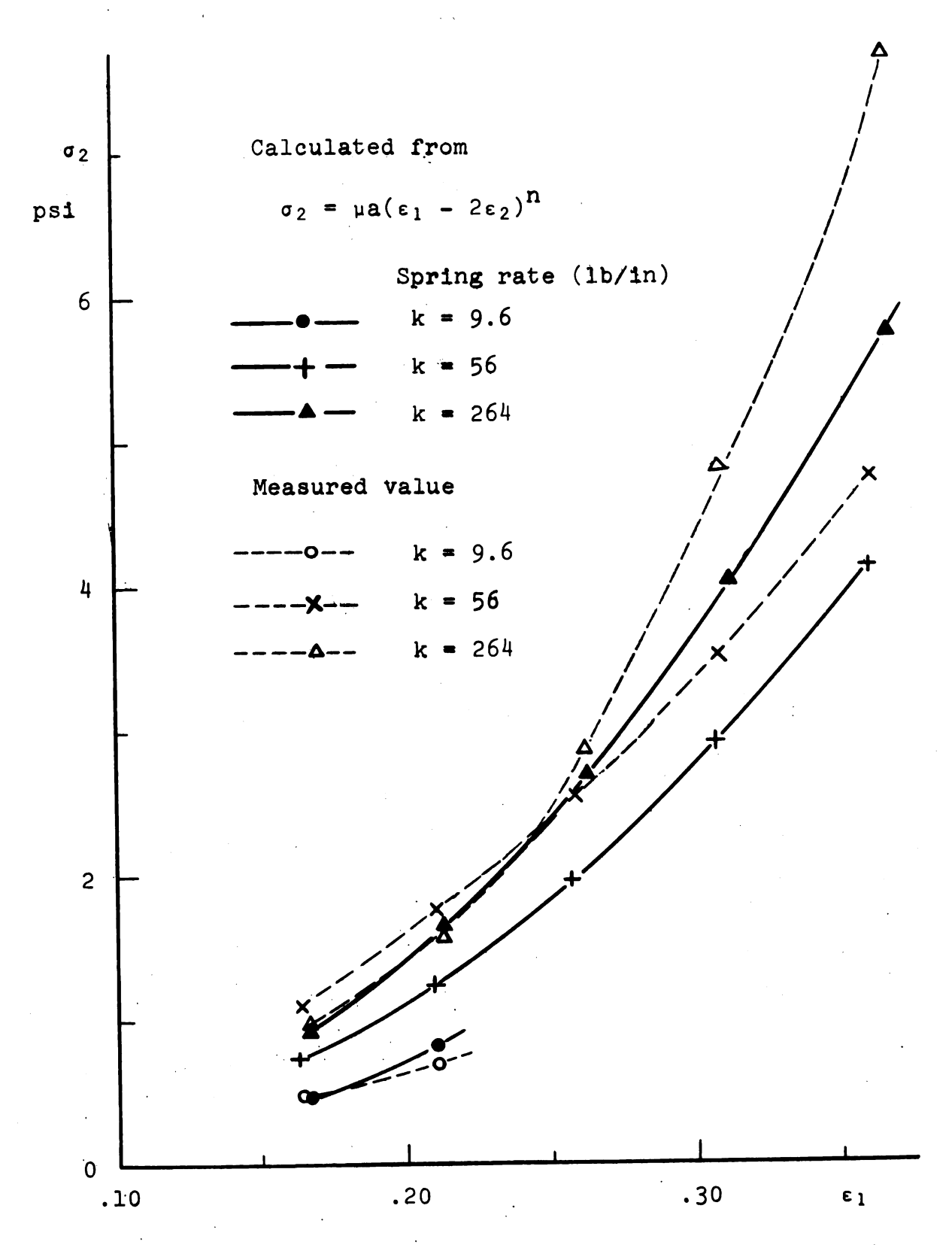


Fig. 7-4. σ_2 from the modified equation (2) $\eta = 1$

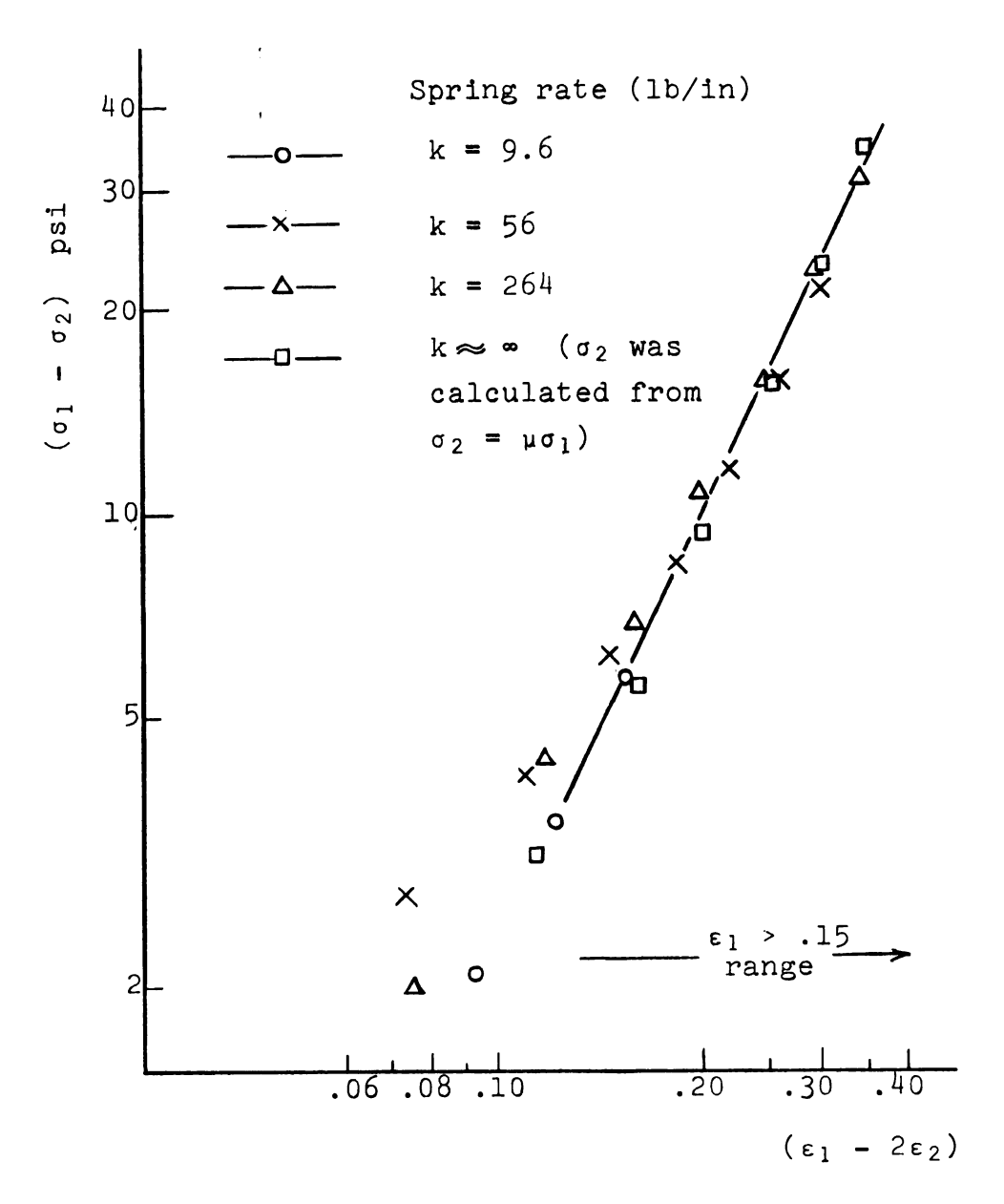


Fig. 7-5. $\log (\sigma_1 - \sigma_2)$ versus $\log (\epsilon_1 - 2\epsilon_2)$ relationship

Other values for η , for example $\eta = \frac{1}{2}$, gives larger deviation from the measured values as shown in Fig. 7-6 and App. C-5.

Thus, eq. (7.14) and eq. (7.15) can be used as F_1 and F_2 functions for the range of ϵ_1 > 0.15. If the initial bulk density is high, these equations could probably be used in the lower range of ϵ_1 also with different values for parameters a and n.

7.2 G Function

As shown in Fig. 6-9, τ is not a function of γ alone, because τ takes various values at the same level of γ . Actually τ seems to be affected by σ_m , which gives a reason to study $\frac{\tau \frac{\pi}{4}}{\sigma_m}$. The values are given in App. C-6. They are fairly constant for all the spring rates with an average value $\frac{\tau \frac{\pi}{4}}{\sigma_m} = 1.00$. $\frac{\tau \pi}{4}$ and σ_m are calculated from eq. (5.8) and eq. (5.11) in which only measured values of σ_1 and σ_2 are used. (The relationship $\sigma_2 = \mu \sigma_1$ is not used.)

The same conclusion is also derived from the relationship σ_2 = $\mu\sigma_1$, because

$$\tau_{\frac{\pi}{4}} = \frac{1}{2}(\sigma_1 - \sigma_2) = \frac{1 - \mu}{2} \sigma_1$$
 (7.17)
$$\sigma_{m} = \frac{\sigma_1 + 2\sigma_2}{3} = \frac{1 + 2\mu}{3} \sigma_1$$

Therefore,

$$\frac{\sigma_{m}}{\sigma_{m}} = \frac{3(1-\mu)}{2(1+2\mu)} \tag{7.18}$$

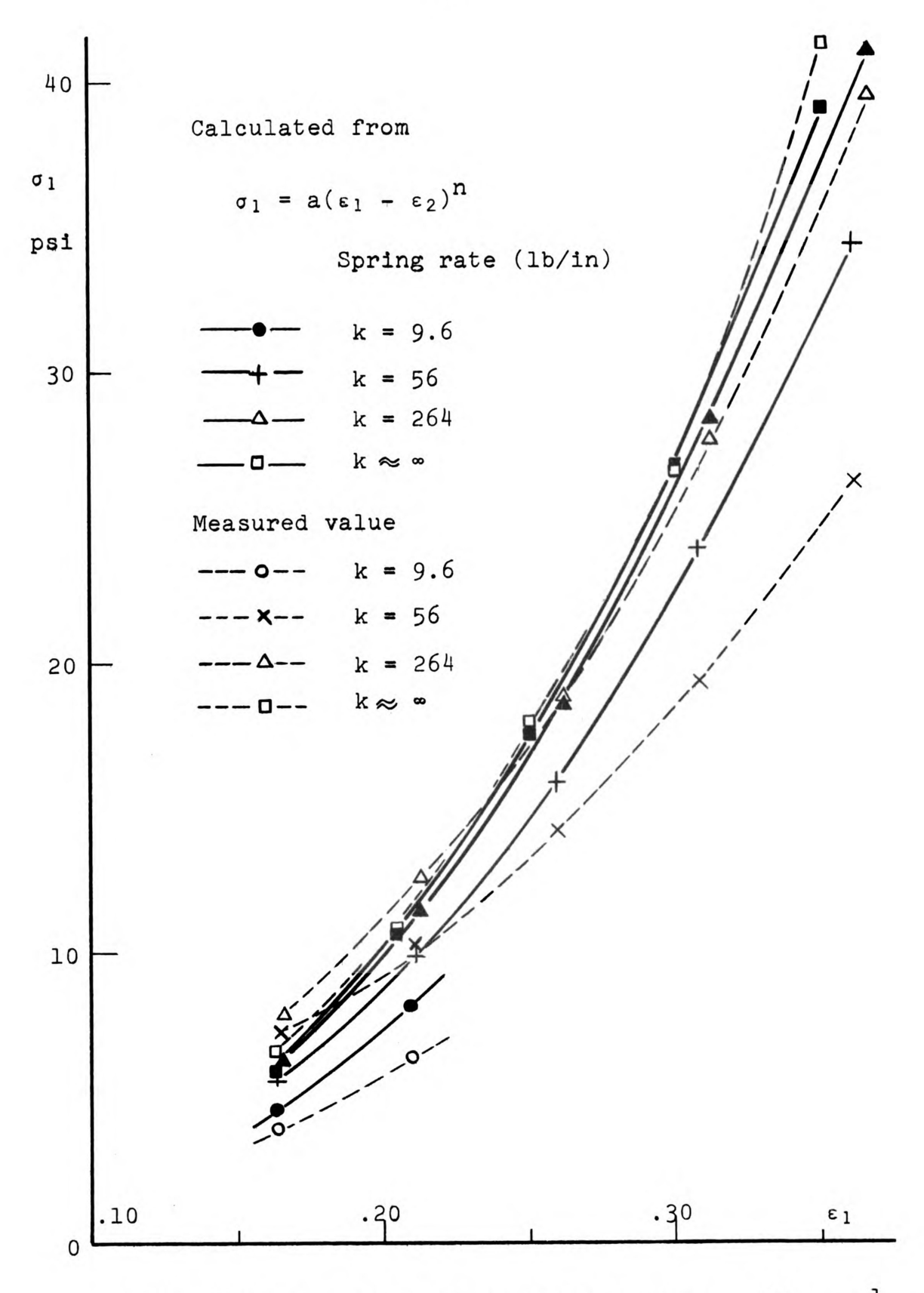


Fig. 7-6. σ_1 from the modified equation (2) $\eta = \frac{1}{2}$

where μ is the average value for all the test range and μ = 0.141.

Hence, $\frac{\tau_{\overline{4}}}{\sigma_{m}} = 1.01$ from eq. (7.18). This agrees naturally with the above calculation. So far as the relationship $\sigma_{2} = \mu \sigma_{1}$ is valid, $\tau_{\overline{4}}$ has a linear relationship with σ_{m} in the form of eq. (7.18).

Since γ is a function of e_1 and e_2 in the form of eq. (5.10), it is possible to express a G function in terms of ϵ_1 and ϵ_2 . Using eq. (7.14) and eq. (7.17), a G function in the following form is obtained.

$$\tau_{\frac{\pi}{4}} = \frac{(1-\mu)}{2} \mathbf{a}(\varepsilon_1 - 2\varepsilon_2)^n \tag{7.19}$$

7.3 <u>H Function</u>

An experimental equation similar to the original consolidation equation is derived in Chapter VI, 6.6.

However, if the relationship between σ_m and $\frac{\Delta V}{V_0}$ should be consistent with eq. (7.14), the following equation (7.20) is derived.

Since
$$\ln(1 + \frac{\Delta V}{V_0}) = 2\varepsilon_2 - \varepsilon_1$$
 (from eq. (5.15))
and $\sigma_m = \frac{1 + 2\mu}{3} a(\varepsilon_1 - 2\varepsilon_2)^n$,
 $\sigma_m = \frac{1 + 2\mu}{3} a\{-\ln(1 + \frac{\Delta V}{V_0})\}^n$ (7.20)

where $\Delta V < 0$ for compression.

In Fig. 7-7, the σ_m values calculated from eq. (7.20) are plotted against the σ_m values which are directly obtained from the measured value of σ_1 and σ_2 . They show a fairly good coincidence considering the large deviation of measured values and of the μ value in the calculation.

 $\sigma_{m} \text{ can be expressed in terms of bulk density } \rho.$ Since $\rho = \frac{W}{V} = \frac{\rho_{0}}{1 + \frac{\Delta V}{V_{0}}} \text{ (accordingly } \frac{\Delta V}{V_{0}} = -\frac{\Delta \rho}{\rho}), \text{ eq. (7.20) becomes}$

$$\sigma_{\rm m} = \frac{1 + 2\mu}{3} \, a \left(\ln \frac{\rho}{\rho_0} \right)^{\rm n} \tag{7.21}$$

7.4 <u>Conventional Strain System and Natural Strain System</u>

In Fig. 7-8, σ_1 is expressed in terms of the conventional strain e_1 , although the strain is expressed as natural strain in all other diagrams in this thesis. A comparison of this figure with Fig. 6-5 shows that Fig. 6.5 may give a slightly clearer idea in dividing the whole function into two straight lines. The difference is, however, almost negligible. Both systems fit to the form of $\sigma_1 = a\varepsilon_1^n$ or $\sigma_1 = ae_1^n$, although the values of a and n are different for each system. Therefore, from the viewpoint of formation of stress-strain relationships, there will be no appreciable difference between the two systems.

Although the conventional strain system has simpler equations in most cases as listed in App. C-8, theoretically speaking, natural strain is better for handling large strain.

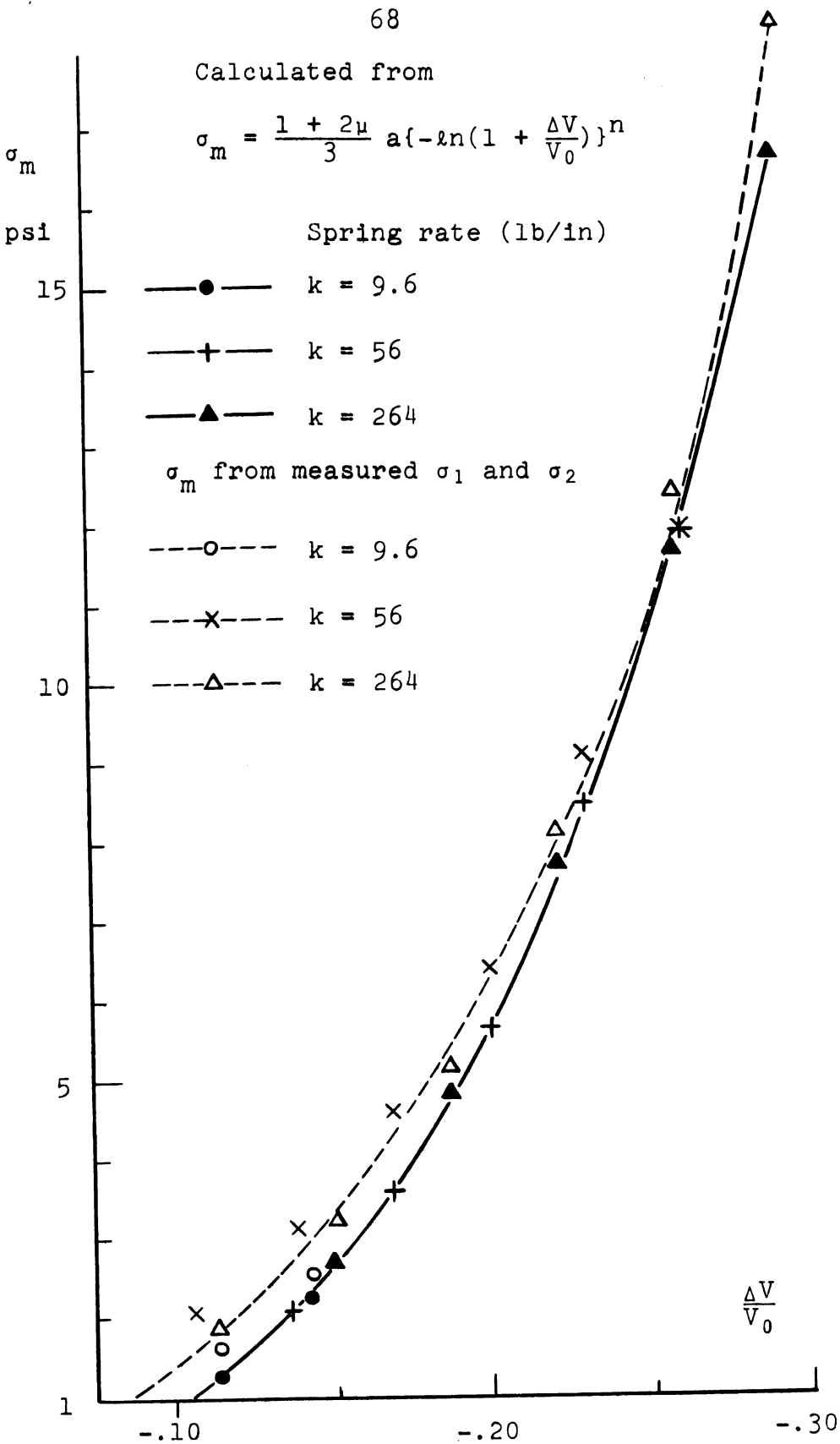


Fig. 7-7. σ_{m} calculated from $\frac{\Delta V}{V_{0}}$.

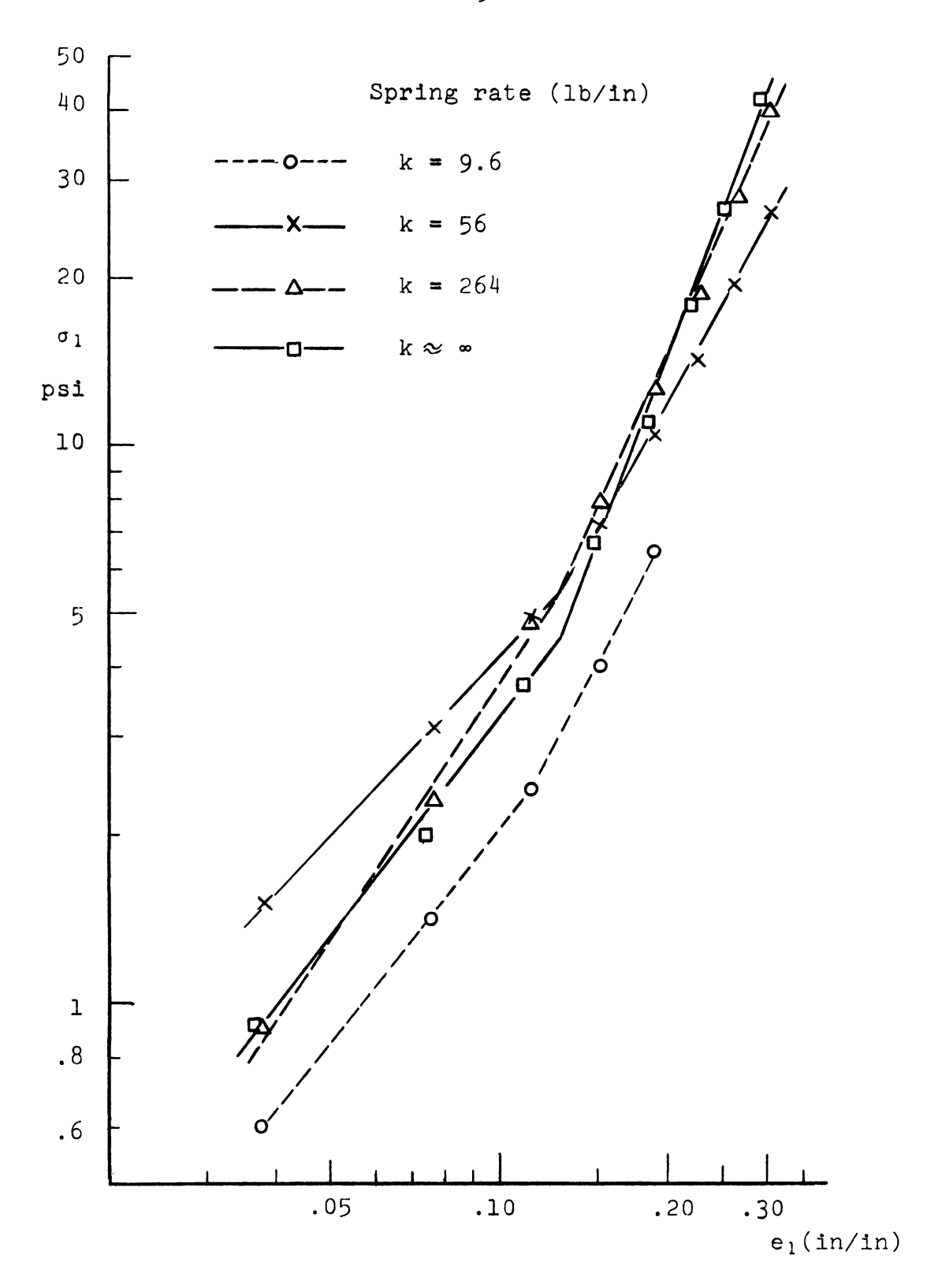


Fig. 7-8.--log σ_1 versus log e_1 relationship.

This is especially true when the volume change or bulk density is handled. The author has, therefore, used natural strain for the theoretical calculations.

VIII. SUGGESTIONS FOR THE APPLICATIONS

1. Method of obtaining parameters

The simplest method to get the three parameters a, n and μ will be a compression test of soil in a thin-walled cylinder on which strain gages are attached to pick up σ_2 under the condition of ε_2 = 0. The wall must be lubricated with friction reducer.

By plotting σ_1 and ε_1 on a log-log chart, a and n are obtained. μ can be calculated from eq. (6.2).

2. Calculation of stress components

If the principal strain components ϵ_1 and ϵ_2 are given, σ_1 , σ_2 and τ can be calculated from equations (7.14), (7.15) and (7.17).

The X-ray technique could be used for measuring the strain in the soil. ϵ_{x} , ϵ_{y} and γ_{xy} are obtained from the deformation of the grid of lead spheres buried in the soil. ϵ_{1} and ϵ_{2} are easily calculated from them.

3. Boundary value problems

Simple force-deformation problems of soil might be solved by a numerical method using the stress-strain relationship together with the equation of stress equilibrium and strain compatibility as well as boundary values. It

might be possible to compute stress-strain distribution by selecting a network over the stress field and calculate the stress-strain values at each node step by step.

4. Simulation type study

A simple approximation method might be possible for those practical problems in which the situation could be simulated by a compression test of soil under certain lateral strain confinement. For example, the problem of soil deformation under the tractor tires might be simulated by this laboratory test of variable lateral confinement.

IX. SUMMARY AND CONCLUSIONS

9.1 Summary

A two-dimensional stress-strain law for soil is required to solve the problems of tillage and traction.

The author studied the behavior of a cylindrical soil sample which was laterally confined with springs of various spring rates. The sample was compressed axially at the rate of 0.092 in/min and the axial stress and strain were measured. The lateral strain was also measured with strain gage transducers. Since the sample was laterally confined by the springs, the lateral stress could be obtained from the known spring rate. The shear stress was calculated from the two normal stresses. The shear strain was measured from X-ray photographs of soil sample in which small lead spheres were buried. The change in the angle of the lines between the spheres corresponds to the shear strain. The shear strain was also calculated from two principal strain components assuming that there was no wall friction.

A loam with an average moisture content of 12.4% dry basis was used. The soil was packed in the cylinder with a pneumatic vibrator. The average initial bulk

density was 0.0346 lb/in³. A friction reducer which was a mixture of grease and graphite was applied inside of the cylinder wall and on the pistons. The wall friction was small enough to satisfy the assumption that the stress distribution was uniform in the sample and that the shear stress on the surface of the sample was negligible.

Four tests were carried out for the various spring rates (lb/in) of 9.6, 56, 264 and ∞ (fixed wall). Three replications were made for each test.

It was first assumed that the functions which described the relationship between principal stresses and principal strains are unique for the loading (compression) process below the failure point. A series of tests gave the following relationships

$$\sigma_1 = F_1(\epsilon_1, \epsilon_2)$$

$$\sigma_2 = F_2(\epsilon_1, \epsilon_2)$$

The functional form of F_1 and F_2 was derived by applying the isotropic hardening theory and by modifying it. They were in the form of power functions.

The maximum shear stress was also formulated in terms of ϵ_1 and $\epsilon_2.$

The functional relationship between mean normal stress σ_m and volume change as well as between σ_m and bulk density change was derived by using F_1 and F_2 functions.

9.2 Conclusions

The following conclusions have been made from this study.

- 1. A soil compression test under various lateral strain confinement has several advantages over a compression test under stress confinement (such as triaxial test) for obtaining stress-strain law below failure point. The advantages are (a) easiness of handling, (b) being able to handle with any kind of soil, (c) more similarity to the actual situation where soil expands laterally under increasing vertical stress, and (d) simpler and lower cost test equipment. The test gives us useful information on stress-strain relationship of soil.
- 2. The effect of wall friction is negligible when a friction reducer is applied properly. The shear strain obtained from X-ray pictures shows good agreement with those values calculated from principal strains on the assumption that there is no wall friction. This implies that expensive X-ray test can be eliminated.
- 3. From a set of tests in which lateral confinement spring rate is changed from almost free expansion to a rigid wall, two graphs showing the relationships $\sigma_1 = F_1(\epsilon_1, \epsilon_2)$ and $\sigma_2 = F_2(\epsilon_1, \epsilon_2)$ have been

obtained. Therefore, principal stresses can be obtained graphically, if principal strains are known (e.g. from X-ray test).

- 4. σ_2/σ_1 = constant (μ) is noticed throughout various lateral strain confinements within this test range of ϵ_1 < 0.36 and ϵ_2 < 0.029.
- 5. A power equation $\sigma_1 = a \varepsilon_1^n$ is valid for the σ_1 versus ε_1 relationship in this test range of $\sigma_1 < 40$ psi. Two straight lines are noticed on the log $\sigma_1 \log \varepsilon_1$ graph.
- 6. By starting from the isotropic hardening theory of metal plasticity and modifying it, the following functional relationships which show fairly good agreement with test results have been derived for the range of $\varepsilon_1 > 0.15$ (bulk density > 0.04 lb/in³).

$$\sigma_1 = a(\epsilon_1 - 2\epsilon_2)^n$$

$$\sigma_2 = \mu a(\epsilon_1 - 2\epsilon_2)^n$$

The three soil parameters a, n and μ can be obtained from a simple fixed wall compression test with lateral pressure pick-up.

7. The maximum shear stress $\tau_{\overline{\Psi}}$ takes various values at the same level of maximum shear strain. $\tau_{\overline{\Psi}}$ seems to be affected by mean normal stress $\sigma_{\overline{m}}$ in the form of

$$\tau_{\frac{\pi}{4}} = \frac{3(1-\mu)}{2(1+2\mu)} \sigma_{m}.$$

 $\tau_{\frac{\pi}{4}}$ could also be formulated in terms of ϵ_1 and ϵ_2 ,

$$\tau_{\frac{\pi}{4}} = \frac{(1-\mu)}{2} a(\epsilon_1 - 2\epsilon_2)^n$$
 for $\epsilon_1 > 0.15$.

8. The functional relationship between mean normal stress and volume change seems to be in the following form from the test results.

$$\log \sigma_{\rm m} = k_0 \cdot \frac{\Delta V}{V_0}$$
 for $\epsilon_1 > 0.15$

However, the following function is obtained by using F_1 and F_2 functions.

$$\sigma_{\rm m} = \frac{1 - 2\mu}{3} \ a \{-\ln(1 + \frac{\Delta V}{V_0})\}^{\rm n}$$

A similar equation is obtained for the relation-ship between $\sigma_{\rm m}$ and bulk density.

9. Theoretically, a natural strain system is better than a conventional strain system for dealing with a large strain. However, no practical difference for the formulation of a stress-strain law is noticed between these systems.

SUGGESTIONS FOR FUTURE STUDY

- 1. Improvement of the test equipment in the following points are desired.
 - (a) Greater ε_2 range
 - (b) More rigid cylinder wall
 - (c) Better lubrication method to get smaller, more uniform and constant effect of wall friction.
- 2. Similar tests should be carried out for other soils of various texture, moisture content and density. Another soil parameter η in the following form might have to be introduced.

$$\sigma_1 = a(\epsilon_1 - 2\eta\epsilon_2)^n$$

$$\sigma_2 = a\mu(\epsilon_1 - 2\eta\epsilon_2)^n$$

3. After part two is studied, a field test equipment similar to the fixed wall test cylinder with μ (and η) pick-up transducers should be developed.

Development of a soil strain transducer is desired.

4. The applications of the stress-strain law should be studied extensively. One of the first examples should be the penetration test which has been used so much as a method of measuring soil strength and deformation.

REFERENCES

- Ahlvin, R. G. and D. N. Brown
 1960. Duplication of prototype stress-strain relationships in soil masses by laboratory tests. Proc.
 ASTM 60. 1137-1150.
- Berezantsev, V. G.

 1955 Limiting loads in the indentation of a cohesive material by spherical and conical punches.

 Translated from Russian. Sci. Inf. Dept. NIAE.
- Cooper, A. W. and M. L. Nichols
 1959 Some observations on soil compaction tests,
 Agr. Engr. 40-5, 264-267.
- Drucker, D. C., et al.
 1957 Soil mechanics and work-hardening theories of plasticity. Trans. ASCE 122:338-346.
- Drucker, D. C.

 1961 On stress-strain relations for soils and loading capacity. Proc. International Conf. on the Mechanics of Soil-Vehicle System No. 1, 15-24.
- Hendrick, J. G. and G. E. VandenBerg

 1961 Strength and energy relations of a dynamically loaded clay soil. Trans. ASAE 4-1, 31-32, 36.
- Hill, R.

 1950 The mathematical theory of plasticity. Oxford Univ. Press.
- Kondner, R. L. and R. J. Krizek

 1964 A vibratory uniaxial compression device for cohesive soil. Proc. ASTM 64, 934-943.
- Lotspeich, F. B.

 1964 Strength and bulk density of compacted mixture of kaolinite and glass beads. Proc. Soil Sci. Soc. 28:737-743.
- McMurdie, J. L.

 1963 Some characteristics of the soil deformation process. Proc. Soil Sci. Soc. 27:251-254.

- Reaves, C. A., and M. L. Nichols
 1955 Surface soil reaction to pressure. Agr. Engr. 36-12, 813-816.
- Roberts, J. E., and J. M. Souza

 1958 The compressibility of sand. Proc. ASTM 58:
 1269-1277.
- Scott, R. F.
 1963 Principles of soil mechanics. Addison-Wesley
 Publ. Co.
- Soehne, W.

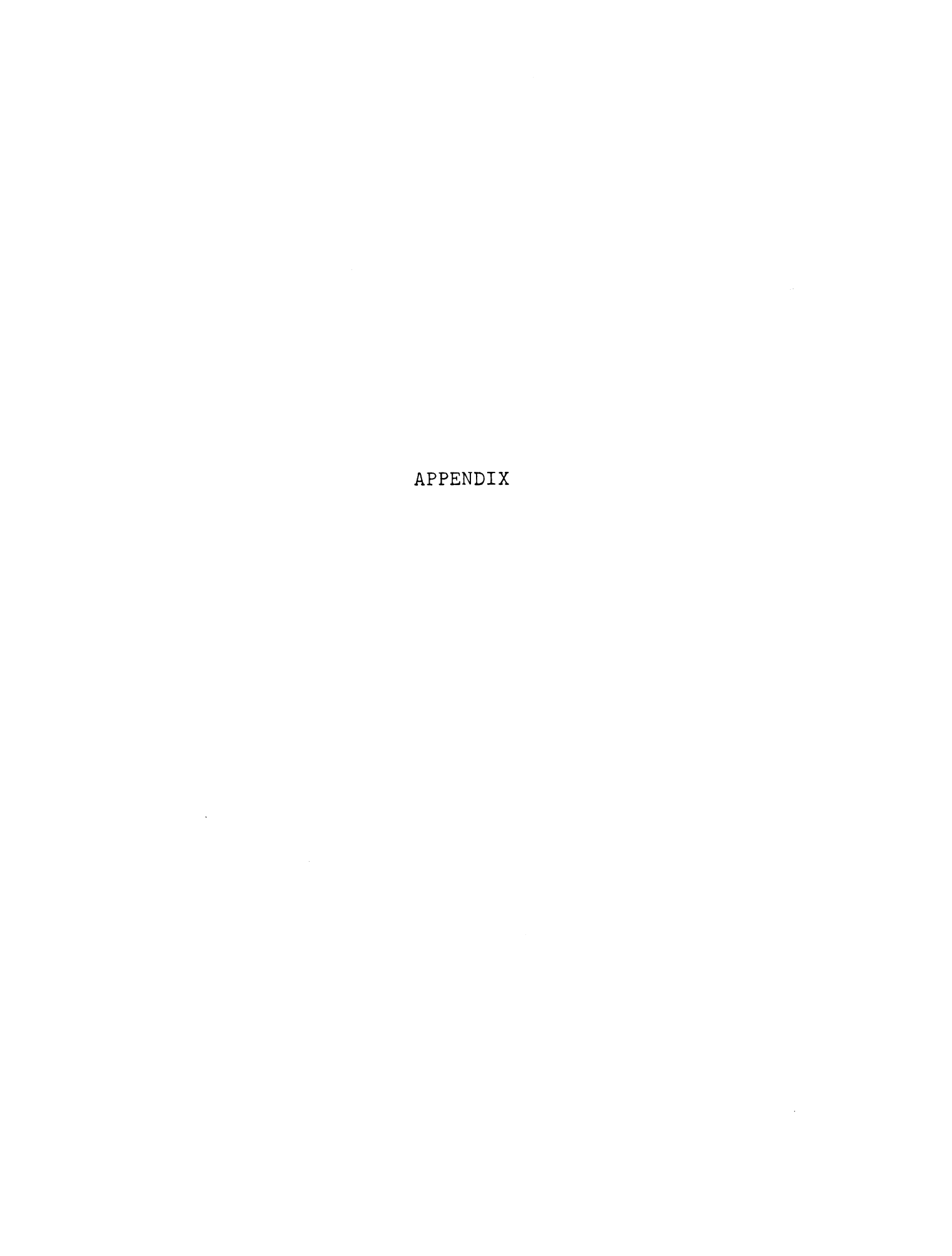
 1956 Einige Grundlagen für eine Landtechnische
 Bodenmechanik. Grundlagen der Landtechnik Hf.
 7, 11-27.
- Soehne, W. H., W. J. Chancellor and R. H. Schmidt
 1959 Soil deformation and compaction during piston
 sinkage. ASAE paper 59-100.
- Taylor, J. H., and G. E. VandenBerg

 1965 The role of displacement in a simple traction system. ASAE paper 65-122.
- VandenBerg, G. E., W. F. Buchele, and L. E. Malvern 1958 Application of continuum mechanics to soil compaction. Mich. Agr. Exp. Sta. Jour. No. 2251.
- VandenBerg, G. E.

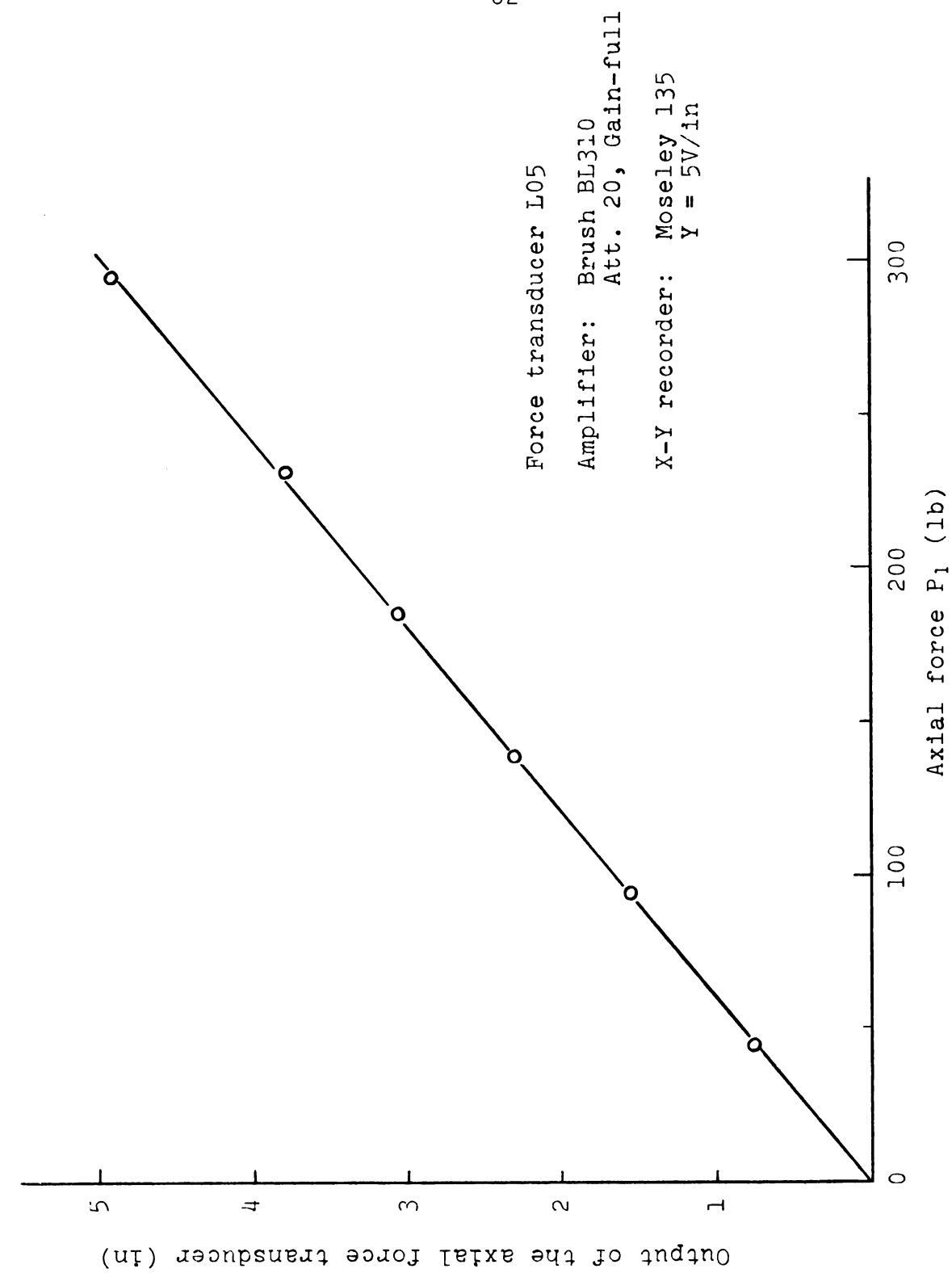
 1962 Triaxial measurements of shearing strain and compaction in unsaturated soil. ASAE paper 62-648.
- Vomocil, J. A., L. J. Waldron, and W. J. Chancellor 1961 Soil tensile strength by centrifugation. Proc. Soil Sci. Soc. 25-3, 176-180.
- Waldron, L. J.

 1964 Soil viscoelasticity; superposition tests.

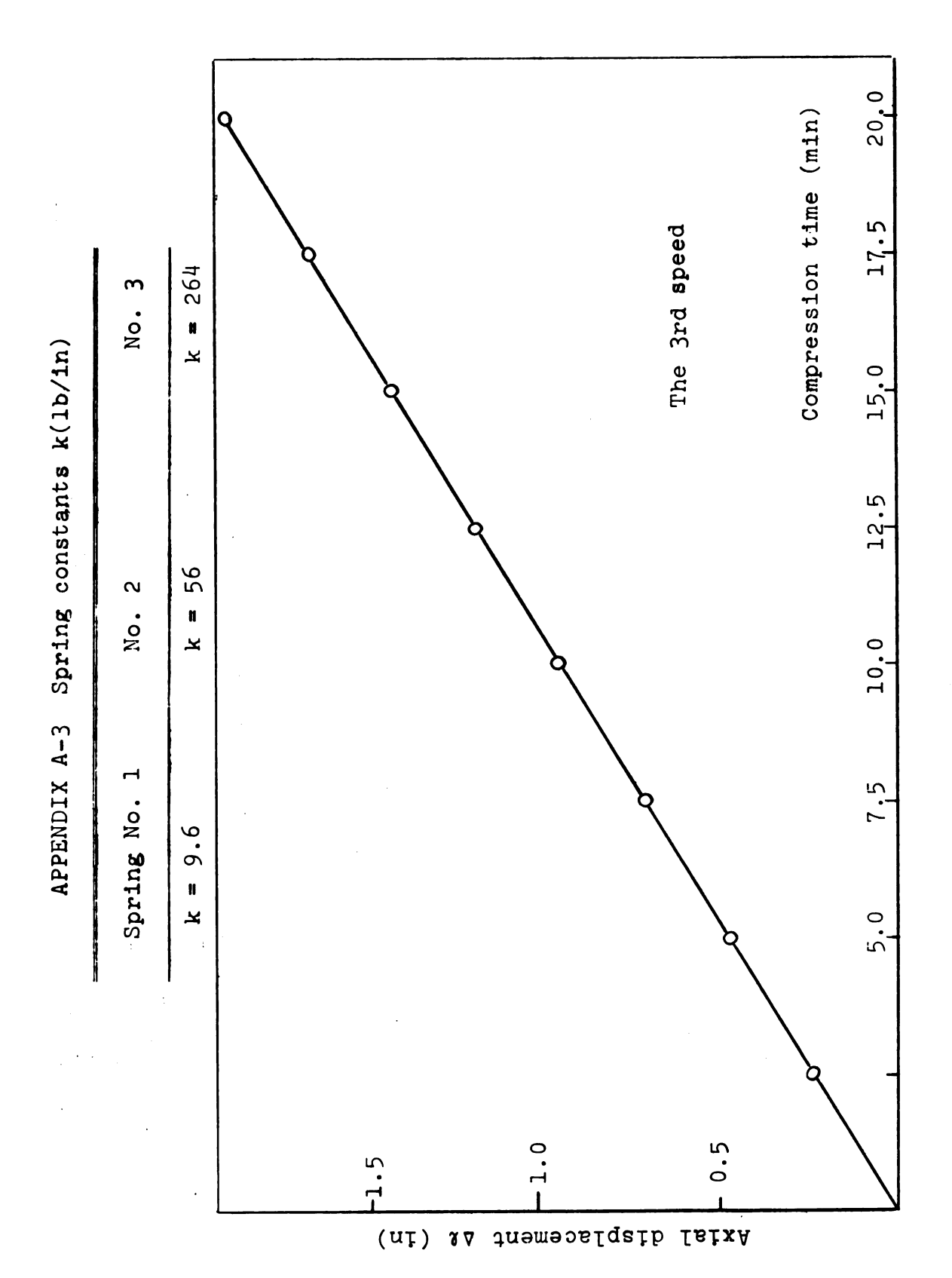
 Proc. Soil Sci. Soc. 28, 323-328.
- 1964 Viscoelastic function for soils. Proc. Soil Sci. Soc. 28, 329-333.
- Waterways Experiment Station
 1952 Torsion shear apparatus and testing procedures.
 WES Bulletin 38, 75.
 - Physical components of the shear strength of saturated clays. WES miscellaneous paper No. 3-428.



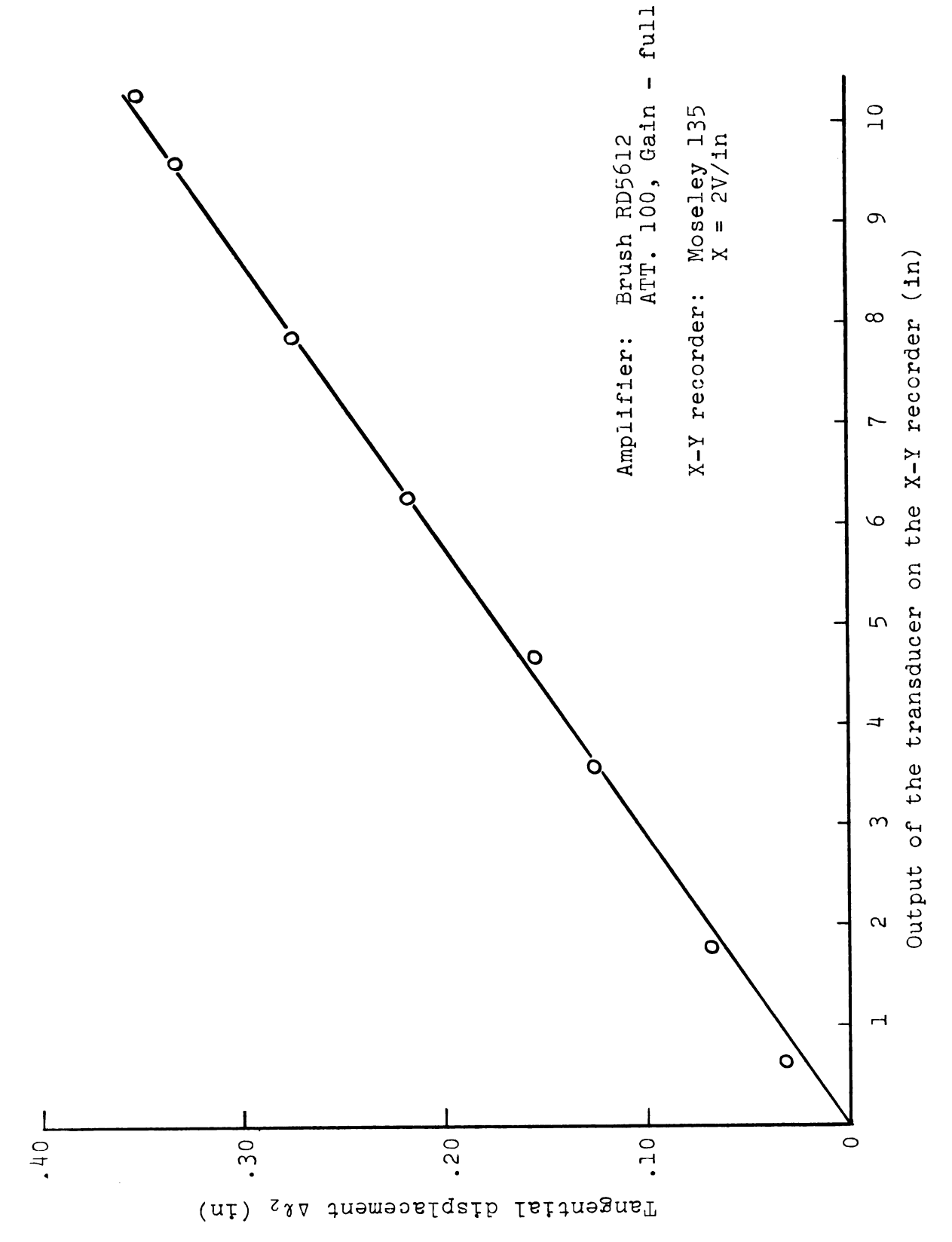




APPENDIX A-1 Calibration chart for axial force transducer



APPENDIX A-2 Calibration of axial displacement of compression piston in terms of time.



APPENDIX A-4 Calibration chart for lateral displacement transducer

APPENDIX B-1

 σ_1 Values (psi) From eq. (5.1)

Δ2	Spi	ring rate	k(lb/in)	
(in)	k = 9.6	k = 56	k - 264	k ~ ∞
0	0	0	0	0
0.23	.60	1.45	.85	.85
0.46	1.35	3.05	2.30	1.98
0.69	2.43	4.90	4.85	3.68
0.92	3.98	7.24	7.94	6.55
1.15	6.37	10.35	12.53	10.99
1.38		14.18	18.85	17.99
1.61		19.38	27.66	26.50
1.84		26.13	39.51	41.27

APPENDIX B-2

(a) e₁ Values (in/in) From eq. (5.2)

۵٤	Spr	Spring rate k(lb/in)			
(in)	k = 9.6	k = 56	k = 264	k ≈ ∞	
0	0	0	0	0	
0.23	.0379	.0379	.0384	.0370	
0.46	.0758	.0758	.0768	.0741	
0.69	.1137	.1137	.1152	.1111	
0.92	.1516	.1516	.1536	.1481	
1.15	.1895	.1895	.1920	.1852	
1.38		.2273	.2304	.2222	
1.61		.2652	.2688	.2593	
1.84		.3031	.3072	.2963	

(b) ϵ_1 Values From eq. (5.3)

Δ l	Spring rate k(lb/in)				
(in)	k = 9.6	k = 56	k = 264	k≈∞	
0	0	0	0	0	
0.23	.0387	.0387	.0391	.0377	
0.46	.0788	.0788	.0798	.0770	
0.69	.1207	.1207	.1224	.1177	
0.92	.1644	.1644	.1668	.1603	
1.15	.2101	.2101	.2132	.2048	
1.38		.2579	.2619	.2513	
1.61		.3082	.3131	.3002	
1.84		.3611	.3670	.3514	

APPENDIX B-3

 σ_2 Values (psi) From eq. (5.4)

A 0	Spring	rate k(lb/in)	
Δl (in)	k = 9.6	k = 56	k = 264
0	0	0	0
0.23	.09	.16	.17
0.46	.21	• 35	.30
0.69	.34	.64	.50
0.92	.48	1.10	.98
1.15	.67	1.78	1.57
1.38		2.54	2.87
1.61		3.52	4.82
1.84		4.74	7.68

APPENDIX B-4

(a)	e 2	Values	(in/in)	From	eq.	(5.5)
-----	-----	--------	---------	------	-----	-------

Δ &	S	pring rat	e k(lb/in)	
(in)	k = 9.6	k = 56	k = 264	k ≈ ∞
0	0	0	0	0
0.23	.0044	.0013	.0003	0
0.46	.0099	.0028	.0005	0
0.69	.0153	.0049	.0008	0
0.92	.0211	.0081	.0015	0
1.15	.0280	.0126	.0023	.0001
1.38		.0172	.0040	.0004
1.61		.0228	.0064	.0010
1.84		.0293	.0097	.0017

(b) ϵ_2 Values From eq. (5.6)

Δ &	S	pring rate	e k(lb/in)	
(in)	k = 9.6	k = 56	k = 264	k ≈ ∞
0	0	0	0	0
0.23	.0044	.0013	.0003	0
0.46	.0099	.0028	.0005	0
0.69	.0152	.0049	.0008	0
0.92	.0209	.0081	.0015	0
1.15	.0276	.0125	.0023	.0001
1.38		.0171	.0040	.0004
1.61		.0226	.0064	.0010
1.84		.0289	.0097	.0017

APPENDIX B-5

(a)	σm	Values	(psi)	From eq.	(5.11)
· — /	- 111		(P /		() (– –)

Δ٤	Sprin	g rate k(lb/i	n)
(in)	k = 9.6	k = 56	k = 264
0	0	0	0
0.23	.26	•59	.40
0.46	•59	1.25	.97
0.69	1.04	2.06	1.95
0.92	1.65	3.15	3.30
1.15	2.57	4.64	5.22
1.38		6.42	8.20
1.61		9.14	12.43
1.84		11.87	18.29

(b) σ_1 , σ_2 Values (psi) From eq. (5.12) and eq. (5.13)

		Sı	pring rat	te k(lb/in)	
۵۱ (in)	k	= 9.6	k	= 56	k	= 264
(111)	σ ₁ '	σ2'	σ ₁ '	σ ₂ '	σι	σ ₂ '
0	0	0	0	0	0	0
0.23	.34	17	.86	43	.45	 23
0.46	.89	45	1,80	 90	1.33	 67
0.69	1.39	70	2.84	-1.42	2.90	-1.45
0.92	2.33	-1.17	4.09	-2.05	4.64	-2.32
1.15	3.80	-1.90	5.71	-2.86	7.31	-3. 65
1.38			7.76	-3.88	10.65	-5.33
1.61			10.57	- 5.29	15.23	-7. 61
1.84			14.26	-7.1 3	21.22	-10.28

APPENDIX B-6

τ_{π}	Values	(psi)	From	eq.	(5.8)
-					

Δ &	Sprin	g rate k(lb/in)
(in)	k = 9.6	k = 56	k = 264
0	0	0	0
0.23	.26	.65	.34
0.46	.67	1.35	1.00
0.69	1.05	2.13	2.18
0.92	1.75	3.07	3.48
1.15	2.85	4.29	5.48
1.38		5.82	7.99
1.61		7.93	11.42
1.84		10.70	15.92

APPENDIX B-7

Values	From eq. (5.10)		
Δ &	Spring	g rate k(lb/in))
(in)	k = 9.6	k = 56	k = 264
0	0	0	0
0.23	.0430	.0400	.0394
0.46	.0882	.0814	.0802
0.69	.1358	.1228	.1228
0.92	.1840	.1714	.1676
1.15	.2356	.2202	.2140
1.38		.2716	.2628
1.61		.3256	.3194
1.84		.3804	.3674

APPENDIX B-8

 $\Delta V/V_0$ Values From eq. (5.14)

<u>Δ</u>	Sprin	ng rate k(lb/in)	
(in)	k = 9.6	k = 56	k = 264
0	0	0	0
0.23	 0294	 0354	0378
0.46	 0575	0706	 0759
0.69	0864	10 50	1138
0.92	1155	 1378	1511
1.15	1435	 1689	1883
1.38		 2005	2243
1.61		 2313	2594
1.84		 2616	2937

APPENDIX B-9

From eq. (6.2) μ Values Calculated from Individual Test

	Spring	Spring rate k	9.6 =	Sprir	Spring rate k	k = 56	Spr	Spring rate	k = 264
۵٤ (in)	No. 1	Test No. 2	No. 3	No. 1	Test No. 2	No. 3	No. 1	Test No. 2	No. 3
0									
0.23	.339	.136	760.	.113	.088	.137	860.	.195	.261
94.0	.271	.155	.115	.123	.109	.116	.078	.105	,224
69.0	.224	.139	901.	.124	.117	.148	.075	680.	.157
0.92	.184	.120	ħ60·	.153	.129	.181	760.	.113	.151
1.15	.153	.114	.088	.188	.145	.198	860.	.133	.155
1.38				.187	.157	.204	.129	.153	.189
1.61				.186	.157	.216	.155	.162	.205
1.84				.184	.157	.220	.178	.184	.225

APPENDIX C-1 $\sigma_1 \text{ Values from Isotropic Hardening Theory}$ $\sigma = a(\epsilon_1^2 - 2\epsilon_2^2)^{\frac{n}{2}} \text{ (psi)}$

Δ٤	Spi	ring rate k	(lb/in)	
(in)	k = 9.6	k = 56	k = 264	k ∞
0.92	6.19	6.29	6.54	5.94
1.15	11.17	11.36	11.82	10.73
1.38		18.61	19.41	17.58
1.61		28.58	29.87	27.00
1.84		41.84	43.81	39.48

APPENDIX C-2

 σ_1 Values from the Modified Equation (1)

$$\sigma_1 = a(\epsilon_1^n - \frac{1}{\mu}\epsilon_2^n)$$
 (psi)

<u>Δ</u> &	Spi	ring rate k	(lb/in)	
(in)	k = 9.6	k = 56	k = 264	k ∞
0.92	6.01	5.96	6.54	5.94
1.15	10.81	11.31	11.82	10.73
1.38		18.54	19.41	17.58
1.61		28.40	29.87	27.00
1.84		41.54	43.81	39.48

APPENDIX C-3

 σ_1 Values from the Modified Equation (2), $\eta=1$ $\sigma_1=a(\epsilon_1-2\epsilon_2)^n \quad \text{(psi)}$

Δ٤	Sp	ring rate k	(lb/in)	
(in)	k = 9.6	k = 56	k = 264	k≈∞
0.92	3.11	4.91	6.26	5.94
1.15	5.47	8.40	11.21	10.70
1.38		13.27	18.02	17.44
1.61		19.62	27.02	26.56
1.84		27.67	38.46	38.57

APPENDIX C-4

 σ_2 Values from the Modified Equation (2), $\eta=1$ $\sigma_2=\mu a(\epsilon_1-2\epsilon_2)^n \quad \text{(psi)}$

Δ٤	Spring rate k(lb/in)			
(in)	k = 9.6	k = 56	k = 264	k≈∞
0.92	0.46	0.73	0.93	0.89
1.15	0.82	1.25	1.67	1.59
1.38		1.98	2.68	2.60
1.6r		2.92	4.03	3.96
1.84		4.12	5.73	5.75

APPENDIX C-5

 σ_1 Values from the Modified Equation (2), $\eta=\frac{1}{2}$ $\sigma_1=a(\epsilon_1-\epsilon_2)^n$ (psi)

Δ٤	Sp	ring rate	k(lb/in)	
(in)	k = 9.6	k = 56	k = 264	k≈ ∞
0.92	4.54	5.59	6.39	5.94
1.15	8.13	9.85	11.51	10.72
1.38		15.85	18.71	17.51
1.61		23.94	28.43	26.78
1.84		34.48	41.11	39.03

APPENDIX C-6

τπ/	σm	Values	

Δ &	Spring	rate k(lb/in	1)
(in)	k = 9.6	k = 56	k = 264
0			
0.23	1.00	1.10	0.85
0.46	1.14	1.08	1.03
0.69	1.01	1.03	1.12
0.92	1.06	0.97	1.05
1.15	1.11	0.92	1.05
1.38		0.91	0.97
1.61		0.87	0.92
1.84		0.90	0.87

APPENDIX C-7

 $\sigma_{\rm m}$ Values calculated from $\frac{\Delta V}{V_0}$, (psi) From eq. (7.20)

Δl (in)	Spring rate k(lb/in)		
	k = 9.6	k = 56	k = 264
0.92	1.35	2.13	2.71
1.15	2.36	3.63	4.85
1.38		5.76	7.79
1.61		8.50	11.69
1.84		11.98	16.65

APPENDIX C-8

Comparison Between Conventional Strain System and Natural Strain System

Natural Strain System $\epsilon_1 = -kn$ = 8n Conventional Strain System **e**₂ e G

 $\sigma_2 = \mu a (e_1 - 2e_2)^n$ $\sigma_1 = a(e_1 - 2e_2)^n$ ⟨

(a, n; not the same value as natural strain system)

 $\gamma_{\frac{\pi}{4}} = 2\{\frac{\pi}{4} - \tan^{-1}(\frac{1-e_1}{1+e_2})\}$ $\tau_{\frac{\pi}{4}} = \frac{\sigma_1 - \sigma_2}{2}$

5

 $\frac{\Delta V}{V_0} = (1 + e_2)^2 (1 - e_1) -$ 9

 $\sigma_2 = \mu a(\epsilon_1 - 2\epsilon_2)^n$

 $2\{\frac{\pi}{4} - \tan^{-1}(e^{-\epsilon_1-\epsilon_2})\}$

or $\ln(\frac{\Delta V}{V_0} + 1) = 2\varepsilon_2$

MICHIGAN STATE UNIV. LIBRARIES
31293003772096